Universal Amplitude Ratios in the Critical Two-Dimensional Ising Model on a Torus

Jesús Salas
Departamento de Física Teórica
Facultad de Ciencias, Universidad de Zaragoza
Zaragoza 50009, SPAIN
JESUS@MELKWEG.UNIZAR.ES

Alan D. Sokal
Department of Physics
New York University
4 Washington Place
New York, NY 10003 USA
SOKAL@NYU.EDU

March 31, 1999
revised October 6, 1999

Abstract

Using results from conformal field theory, we compute several universal amplitude ratios for the two-dimensional Ising model at criticality on a symmetric torus. These include the correlation-length ratio $x^\star = \lim_{L\to\infty} \xi(L)/L$ and the first four magnetization moment ratios $V_{2n} = \langle \mathcal{M}^{2n} \rangle / \langle \mathcal{M}^2 \rangle^n$. As a corollary we get the first four renormalized $2n$-point coupling constants for the massless theory on a symmetric torus, G^*_{2n}. We confirm these predictions by a high-precision Monte Carlo simulation.

Key Words: Ising model; universal amplitude ratios; conformal field theory; torus; finite-size scaling; corrections to scaling; Monte Carlo; Swendsen–Wang algorithm; cluster algorithm.

1 Introduction

A central concept in the theory of critical phenomena is the idea of *universality*, which states that phase-transition systems can be divided into a relatively small number of "universality classes" (determined primarily by the system's spatial dimensionality and the symmetries of its order parameter) within which certain features of critical behavior are universal. In the 1950s and 1960s it came to be understood that critical exponents are universal in this sense [1]. Later, in the 1970s, it was learned that certain dimensionless ratios of critical amplitudes are also universal [2].

The past quarter-century has seen enormous progress in the determination of critical exponents for a wide variety of universality classes, including exact analytical results for two-dimensional (2D) models [3, 4, 5, 6] and increasingly precise numerical determinations for three-dimensional models by a variety of techniques (field-theoretic renormalization group [7, 8], series extrapolation [9, 10, 11, 12, 13, 14, 15, 16], Monte Carlo [17, 18, 19, 20, 21, 22, 23, 24, 25, 26]). As a result, attention has turned quite naturally to universal amplitude ratios: these include amplitude ratios in infinite volume and those in finite-size scaling (FSS). Though much numerical work has been done, few exact results are known.[1]

The critical behavior of many 2D models can be studied analytically using conformal field theory (CFT) [4, 5, 6]. Many critical exponents have been determined exactly, along with a few universal amplitude ratios [52, 53, 54, 55, 56, 57, 58, 59, 60, 61, 62, 63, 38]. The main goal of the present paper is to compute, using CFT, a few more universal amplitude ratios for the 2D Ising model and to test these predictions by a high-precision Monte Carlo study. The amplitude ratios considered here arise in finite-size scaling; they can be computed starting from the correlation functions of the critical 2D Ising model on a torus.

The first class of quantities we study concern the shape of the magnetization distribution $\rho(\mathcal{M})$ at criticality on a symmetric torus ($L_x = L_y$).[2] We study the rescaled shape of this distribution (i.e. normalizing by its width $\langle \mathcal{M}^2 \rangle^{1/2}$) as well as the dimensionless ratios of its moments,

$$V_{2n} \;=\; \frac{\langle \mathcal{M}^{2n} \rangle}{\langle \mathcal{M}^2 \rangle^n} \;. \tag{1.1}$$

We can also define the dimensionless cumulants

$$U_{2n} \equiv \frac{\langle \mathcal{M}^{2n} \rangle_{\text{conn}}}{\langle \mathcal{M}^2 \rangle^n} \;. \tag{1.2}$$

[1] Among the models studied are the 2D Ising model [27, 28, 29, 30, 31], 2D nonlinear σ-models [32, 33, 34, 28, 29, 35, 36], 2D Potts models [37, 38], the Baxter 8-vertex model [39], 2D and 3D self-avoiding walks [19], the 3D Ising model [40, 41, 20, 42, 43, 27, 44, 45, 28, 29, 46, 24, 25, 31, 26], 3D $O(N)$ spin models [18, 47, 48, 28, 29, 16, 49, 50], 3D site percolation [25], and the 5D Ising model [51]. This list of references is far from exhaustive.

[2] One of the insights of conformal field theory is that universal finite-size-scaling properties (such as the universal amplitude ratios considered here) ought to be studied as analytic functions of the modular parameter τ of the torus. Nevertheless, we think that the case of a symmetric torus ($\tau = i$) is of sufficient practical importance in Monte Carlo simulations to warrant special attention.

For any symmetric distribution $\rho(\mathcal{M}) = \rho(-\mathcal{M})$ these satisfy[3]

$$\begin{aligned} U_4 &= V_4 - 3 && (1.3a)\\ U_6 &= V_6 - 15V_4 + 30 && (1.3b)\\ U_8 &= V_8 - 28V_6 - 35V_4^2 + 420V_4 - 630 && (1.3c)\\ U_{10} &= V_{10} - 45V_8 - 210V_4V_6 + 1260V_6 + 3150V_4^2 - 18900V_4 + 22680 && (1.3d)\\ &\vdots \end{aligned}$$

Note that V_4 and U_4 are closely related to the so-called Binder cumulant [64]

$$U_{4,\mathrm{Binder}} \equiv 1 - \frac{\langle \mathcal{M}^4 \rangle}{3\langle \mathcal{M}^2 \rangle^2} = 1 - \frac{V_4}{3} = -\frac{U_4}{3} \,. \tag{1.4}$$

For $\beta < \beta_c$ the ratios V_{2n} tend in the infinite-volume limit to those characteristic of a Gaussian distribution,

$$\begin{aligned} V_{2n}(\mathrm{Gaussian}) &= (2n-1)!! && (1.5a)\\ U_{2n}(\mathrm{Gaussian}) &= 0 && (1.5b) \end{aligned}$$

while for $\beta > \beta_c$ they tend to those characteristic of a sum of two delta functions,

$$\begin{aligned} V_{2n}(\text{two deltas}) &= 1 && (1.6a)\\ U_{2n}(\text{two deltas}) &= \frac{2^{2n-1}(2^{2n}-1)}{n}\, B_{2n} && (1.6b) \end{aligned}$$

where $B_{2n} = (-1)^{n-1}(2n)!\,\zeta(2n)/2^{2n-1}\pi^{2n}$ is a Bernoulli number. At $\beta = \beta_c$, however, these ratios acquire non-trivial values in-between (1.5a) and (1.6a).[4] These values, which are universal, can in principle be computed by integrating the spin correlators for the critical 2D Ising model on a torus, which were determined by Di Francesco *et al.* [53, 54] using CFT. In practice, however, the formula for V_{2n} rapidly gets more complicated as n grows. Di Francesco *et al.* [53, 54] computed V_4 to roughly three decimal places by Monte Carlo integration. Here we shall improve this result by three orders of magnitude, and shall also compute V_6 to five decimal places, V_8 to almost four decimal places, and V_{10} to three decimal places:

$$\begin{aligned} V_4 &= 1.1679229 \pm 0.0000047 && (1.7)\\ V_6 &= 1.4556491 \pm 0.0000072 && (1.8)\\ V_8 &= 1.89252 \pm 0.00018 && (1.9)\\ V_{10} &= 2.53956 \pm 0.00034 && (1.10) \end{aligned}$$

[3] These relations can be computed from the generating functions

$$\sum_{n=1}^{\infty} \frac{U_{2n}}{(2n)!} z^{2n} = \log\left(\sum_{n=0}^{\infty} \frac{V_{2n}}{(2n)!} z^{2n} \right)$$

with $V_0 = V_2 = 1$ and $V_{2n+1} = 0$.

[4] The Schwarz inequality implies that $V_{2n} \geq 1$ for any model, and the Gaussian inequality [65, 66] implies that $V_{2n} \leq (2n-1)!!$ for ferromagnetic Ising models. In particular, we have $-2 \leq U_4 \leq 0$. Moreover, Newman [67] and Shlosman [68] have proven, for ferromagnetic Ising models, that $(-1)^{n-1}U_{2n} \geq 0$ for all n; and Newman [67] has proven some additional inequalities on the U_{2n}.

Finally, we shall measure the ratios V_{2n} for $2 \le n \le 10$ by Monte Carlo simulation, with an accuracy that gradually deteriorates as n grows. For $n = 2, 3, 4, 5$ our Monte Carlo estimates agree well with the theoretical predictions (but are of course less precise).

Another interesting quantity is the second-moment correlation length ξ. It has a sensible definition in finite volume (see Section 3), and its expected FSS behavior is

$$\xi \;\sim\; L\left[x^\star + AL^{-\Delta} + \cdots\right] , \tag{1.11}$$

where the leading coefficient

$$x^\star \;=\; \lim_{L\to\infty} \xi/L \tag{1.12}$$

is universal.[5,6] Here we shall compute $x^\star$ for the 2D Ising model at criticality by numerically integrating the known spin correlators [53, 54]; we find

$$x^\star \;=\; 0.9050488292 \pm 0.0000000004 \, . \tag{1.13}$$

Our Monte Carlo data confirm this prediction. To our knowledge, this is the first exact determination of $x^\star$ for any universality class. Monte Carlo estimates of $x^\star$ are available for many other 2D models — including the 3-state Potts model [75], the 4-state Potts model [76, 77], the 3-state square-lattice Potts antiferromagnet [78, 79], the XY model [80], and several points on the self-dual curve of the symmetric Ashkin–Teller model [76] — and it would be very interesting to compute $x^\star$ analytically for some of these models. Numerical estimates of $x^\star$ are also available for some three-dimensional spin models [18, 41, 47, 24].

Consider, finally, the dimensionless renormalized four-point coupling constant

$$g_4 \;=\; -\frac{\bar{u}_4}{\chi^2 \xi^d} \;=\; -\frac{U_4}{(\xi/L)^d} \, , \tag{1.14}$$

where $\bar{u}_4$ is the connected four-point function at zero momentum. In the FSS limit $L \to \infty$, $\beta \to \beta_c$ with ξ/L fixed, g_4 is a nontrivial function of the FSS variable ξ/L:

$$g_4 \;=\; F_{g_4}(\xi/L) \, . \tag{1.15}$$

Therefore, the function $g_4(\beta, L)$ fails to be jointly continuous at $(\beta, L) = (\beta_c, \infty)$; many limiting values are possible depending on the mode of approach, and the massive and massless scaling limits

$$g_4^* \;=\; \lim_{\beta\uparrow\beta_c} \lim_{L\to\infty} g_4(\beta, L) \tag{1.16}$$

$$G_4^* \;=\; \lim_{L\to\infty} \lim_{\beta\uparrow\beta_c} g_4(\beta, L) \;=\; \lim_{L\to\infty} g_4(\beta_c, L) \tag{1.17}$$

[5] The quantity $x^\star$ also plays an important role in a recently developed method for extrapolating finite-volume Monte Carlo data to infinite volume [69, 70, 71, 34, 72].

[6] An analogous situation holds in a cylindrical ($L \times \infty$) geometry for the exponential correlation length in the longitudinal direction, $\xi_{exp}(L)$ [which can be defined in terms of the logarithm of the ratio of the two largest eigenvalues of the transfer matrix]. Privman and Fisher [73] showed that $\lim_{L\to\infty} \xi_{exp}(L)/L$ at criticality is universal, and Cardy [74] showed that for 2D conformal-invariant systems it is equal to $1/(\pi\eta)$.

correspond to the two extreme cases $g_4^* = F_{g_4}(0)$, $G_4^* = F_{g_4}(x^\star)$. As a corollary of our computation of V_4 and $x^\star$, we obtain the value of g_4 at criticality on a symmetric torus:

$$G_4^* \;=\; -\frac{U_4}{x^{\star 2}} \;=\; 2.2366587 \pm 0.0000057\,. \tag{1.18}$$

More generally, consider the dimensionless renormalized $2n$-point coupling constant

$$g_{2n} \;=\; \frac{\chi^n\,\bar\Gamma_{2n}}{\xi^{(n-1)d}}\,, \tag{1.19}$$

where $\bar\Gamma_{2n}$ is the amputated one-particle-irreducible $2n$-point function at zero momentum.[7] We can predict the next three renormalized coupling constants at criticality on a symmetric torus:

$$G_6^* \;=\; -\frac{U_6 - 10U_4^2}{x^{\star 4}} \;=\; 29.25457 \pm 0.00015 \tag{1.20a}$$

$$G_8^* \;=\; -\frac{U_8 - 56U_4U_6 + 280U_4^3}{x^{\star 6}} \;=\; 942.6095 \pm 0.0072 \tag{1.20b}$$

$$G_{10}^* \;=\; -\frac{U_{10} - 120U_4U_8 - 126U_6^2 + 4620U_4^2U_6 - 15400U_4^4}{x^{\star 8}} \;=\; 56110.24 \pm 0.56 \tag{1.20c}$$

In addition, we shall provide Monte Carlo estimates of G_{12}^* through G_{20}^* [cf. (4.20) below].

This paper is organized as follows: In Section 2 we review the relevant exact results available for the 2D Ising model at criticality on a torus, and we compute (by numerical integration) the CFT prediction for the quantities $x^\star$, V_4, V_6, V_8 and V_{10}. In Section 3 we explain the Monte Carlo algorithm we have used to simulate this model. In Section 4 we analyze our numerical results for the static observables and compare them against the available exact results. Finally, in Section 5 we present our final conclusions and discuss prospects for future work. In Appendix A we explain how we carried out the numerical integrations involved in computing $x^\star$, and in Appendix B we summarize the definitions and principal properties of the Jacobi theta functions.

2 Theoretical Results

The universal amplitudes we consider in this paper ($x^\star$ and V_{2n}) can be written in terms of integrals of the $2n$-point spin correlation functions of the the critical 2D Ising

[7] The $\bar\Gamma_{2n}$ are defined by the generating-function relation

$$\sum_{n=1}^\infty \frac{\bar\Gamma_{2n}}{(2n)!}\phi^{2n} \;=\; \sup_J \left[J\phi - \sum_{n=1}^\infty \frac{\bar u_{2n}}{(2n)!} J^{2n} \right]\,.$$

Recall that $\bar u_2 = \chi$ and that $\bar u_{2n} = L^{-d}\langle \mathcal{M}^{2n}\rangle_{\rm conn}$.

continuum field theory on a torus. These correlators were obtained by Di Francesco *et al.* [53, 54] using an approach based on conformal field theory. The result is[8]

$$\langle \sigma_{z_1} \cdots \sigma_{z_{2n}} \rangle \;=\; \frac{\sum_{\nu=1}^4 Z_\nu \langle \sigma_{z_1} \cdots \sigma_{z_{2n}} \rangle_\nu}{\sum_{\nu=1}^4 Z_\nu} \tag{2.1}$$

where

$$Z_\nu \;=\; \frac{|\theta_\nu(0)|}{2|\eta|} \tag{2.2}$$

and

$$Z_\nu^2 \langle \sigma_{z_1} \cdots \sigma_{z_{2n}} \rangle_\nu^2 \;=\; \frac{1}{2^{n+2}|\eta|^2} \sum_{\substack{\epsilon_j = \pm 1 \\ \sum_j \epsilon_j = 0}} \left| \theta_\nu\left(\frac{\sum_j \epsilon_j z_j}{2} \right) \right|^2 \prod_{i<j} \left| \frac{\theta_1(z_i - z_j)}{\theta_1'(0)} \right|^{\epsilon_i \epsilon_j / 2} \tag{2.3a}$$

$$\;=\; \frac{\theta_1'(0)^{n/2}}{2^{n+2}|\eta|^2} \sum_{\substack{\epsilon_j = \pm 1 \\ \sum_j \epsilon_j = 0}} \left| \theta_\nu\left(\frac{\sum_j \epsilon_j z_j}{2} \right) \right|^2 \prod_{i<j} |\theta_1(z_i - z_j)|^{\epsilon_i \epsilon_j / 2} \tag{2.3b}$$

Here we have used the complex-number notation $z = x_1 + i x_2$; $\theta_1'(0) \approx 2.8486946040$ is the derivative of $\theta_1(z,\tau)$ with respect to z evaluated at $z = 0$ and $\tau = i$; and $\eta \approx 0.7682254223$ is the usual Dedekind function $\eta(\tau)$ evaluated at $\tau = i$. Please note that $\theta_1'(0) = 2\pi\eta^3$ [cf. (B.13)]. Note also that the contribution of $\{\epsilon_j\}$ to (2.3) is equal to that of $\{-\epsilon_j\}$, so in the numerical evaluation of this expression we need only take half the terms. The expression (2.1) gives the FSS limit for the Ising-model correlation functions at criticality: here z_i denotes the position in lattice units divided by the lattice linear size L.

Remark. Although the sector $\nu = 1$ does not contribute to the partition function [since $Z_1 \sim \theta_1(0) = 0$], it does contribute to the correlation functions [since $Z_1 \langle \sigma_{z_1} \cdots \sigma_{z_{2n}} \rangle_1 \neq 0$]. So this sector cannot simply be discarded. See ref. [53] for details.

The two correlators that are needed in the evaluation of the Binder cumulant are

$$Z_\nu \langle \sigma_{z_1} \sigma_{z_2} \rangle_\nu \;=\; \frac{|\theta_1'(0)|^{1/4}}{2|\eta|} \frac{\left| \theta_\nu\left(\frac{z_1 - z_2}{2} \right) \right|}{|\theta_1(z_1 - z_2)|^{1/4}} \tag{2.4}$$

$$Z_\nu \langle \sigma_{z_1} \sigma_{z_2} \sigma_{z_3} \sigma_{z_4} \rangle_\nu \;=\; \frac{|\theta_1'(0)|^{1/2}}{2\sqrt{2}|\eta|} \left\{ \left| \theta_\nu\left(\frac{z_1 + z_2 - z_3 - z_4}{2} \right) \right|^2 \right.$$

[8] There is a misprint in the normalization of the 4-spin correlator in equation (9) of [54], and in the normalization of the $2n$-spin correlator in equation (6.6) of [53]. We have rederived both correlators using the chiral bosonization prescription presented in [53]. With the correct normalization, shown in (2.1)–(2.3) below, we are able to reproduce the numerical value of V_4 reported in [54], as well as the numerical estimates of V_4, V_6, V_8 and V_{10} obtained in our simulation.

$$\times \left| \frac{\theta_1(z_1 - z_2)\theta_1(z_3 - z_4)}{\theta_1(z_1 - z_3)\theta_1(z_1 - z_4)\theta_1(z_2 - z_3)\theta_1(z_2 - z_4)} \right|^{1/2}$$
$$+ (2 \leftrightarrow 3) + (2 \leftrightarrow 4) \Big\}^{1/2} \tag{2.5}$$

We also need the 6-point correlator to compute V_6. Its exact expression can be deduced easily from the general equation (2.3):

$$Z_\nu \langle \sigma_{z_1}\sigma_{z_2}\sigma_{z_3}\sigma_{z_4}\sigma_{z_5}\sigma_{z_6}\rangle_\nu = \frac{|\theta_1'(0)|^{3/4}}{4|\eta|} \Bigg\{ \left| \theta_\nu\Big(\frac{z_1 + z_2 + z_3 - z_4 - z_5 - z_6}{2} \Big) \right|^2$$
$$\times \Psi(z_1, z_2, z_3, z_4, z_5, z_6) + (2 \leftrightarrow 4) + (2 \leftrightarrow 5) + (2 \leftrightarrow 6)$$
$$+ (3 \leftrightarrow 4) + (3 \leftrightarrow 5) + (3 \leftrightarrow 6) + (2 \leftrightarrow 4; 3 \leftrightarrow 5)$$
$$+ (2 \leftrightarrow 4; 3 \leftrightarrow 6) + (2 \leftrightarrow 5; 3 \leftrightarrow 6) \Bigg\}^{1/2} \tag{2.6}$$

where the function Ψ is defined as

$$\Psi(z_1, z_2, z_3, z_4, z_5, z_6) = \left(\frac{\theta_1(z_{12})\theta_1(z_{13})\theta_1(z_{23})\theta_1(z_{45})\theta_1(z_{46})\theta_1(z_{56})}{\prod_{i=1,2,3;j=4,5,6} \theta_1(z_{ij})} \right)^{1/2} \tag{2.7}$$

and we have used the shorthand notation $z_{ij} \equiv z_i - z_j$.

From these equations we can obtain the values of $x^\star = \lim_{L\to\infty} \xi/L$ and V_{2n} by numerical integration. In particular, the correlation length on a periodic lattice of size L is defined to be

$$\xi \;=\; \frac{1}{2\sin(\pi/L)} \left(\frac{\chi}{F} - 1 \right)^{1/2} \;, \tag{2.8}$$

where χ is the susceptibility (i.e., the Fourier-transformed two-point correlation function at zero momentum) and F is the corresponding quantity at the smallest nonzero momentum $(2\pi/L, 0)$ [see (3.7)/(3.9) and (3.14)/(3.17) below for details]. This is a finite-lattice generalization of the second-moment correlation length. Then, the universal amplitude $x^\star$ is given by

$$x^\star \;=\; \frac{1}{2\pi} \left(\frac{\chi}{F} - 1 \right)^{1/2} \tag{2.9}$$

where

$$\chi \;\sim\; \int d^2z \, \langle \sigma_0 \sigma_z \rangle \tag{2.10}$$
$$F \;\sim\; \int d^2z \, \langle \sigma_0 \sigma_z \rangle \, \cos(2\pi x_1) \tag{2.11}$$

and $\int d^2z = \int_0^1 \int_0^1 dx_1 \, dx_2$. The details of this computation are given in Appendix A. We obtain

$$\int d^2z \, \langle \sigma_0 \sigma_z \rangle \;=\; 1.55243295465 \pm 0.00000000004 \tag{2.12}$$

$$\int d^2z \, \langle \sigma_0 \sigma_z \rangle \, \cos(2\pi x_1) \;=\; 0.04656744682 \pm 0.00000000004 \tag{2.13}$$

As a result, we obtain $x^\star$ with 10 digits of precision:

$$x^\star = 0.9050488292 \pm 0.0000000004 \; . \tag{2.14}$$

We repeated the computation requiring 11 digits of precision in the integrals, and the result was the same.

The universal moment ratio V_4 is given by

$$V_4 \;=\; \frac{\int d^2 z_2 \, d^2 z_3 \, d^2 z_4 \, \langle \sigma_0 \sigma_{z_2} \sigma_{z_3} \sigma_{z_4} \rangle}{\left[\int d^2 z \, \langle \sigma_0 \sigma_z \rangle \right]^2} \; . \tag{2.15}$$

Di Francesco *et al.* [53, 54] performed the integrals in numerator and denominator by Monte Carlo and obtained

$$V_4 \;=\; 1.168 \pm 0.005 \; . \tag{2.16}$$

We have improved this value, as follows: For the denominator of (2.15), we use the very precise estimate (2.12) coming from deterministic numerical integration. For the numerator, we performed a Monte Carlo integration using 10^9 measurements. Our result is

$$V_4 \;=\; 1.1679229 \pm 0.0000047 \; , \tag{2.17}$$

which is compatible with (2.16) but three orders of magnitude more precise. This value also agrees closely with the estimate of Kamieniarz and Blöte [81] based on extrapolation of the exact results (computed by transfer-matrix methods) for $L \le 17$:

$$V_4 \;=\; 1.1679296 \pm 0.0000014 \; , \tag{2.18}$$

where the error bar is of course somewhat subjective.[9]

More generally, the universal moment ratio V_{2n} is given by

$$V_{2n} \;=\; \frac{\int d^2 z_2 \, \cdots \, d^2 z_{2n} \, \langle \sigma_0 \sigma_{z_2} \cdots \sigma_{z_{2n}} \rangle}{\left[\int d^2 z \, \langle \sigma_0 \sigma_z \rangle \right]^n} \; . \tag{2.19}$$

We have been able to compute the (exact except for the numerical integration) values of the ratios V_6, V_8 and V_{10}. We performed the integrals in the numerator by Monte Carlo, using 10^9 measurements for V_6, 4×10^6 measurements for V_8 and 2.5×10^6 measurements for V_{10}. We obtain

$$V_6 \;=\; 1.4556491 \pm 0.0000072 \tag{2.20}$$

$$V_8 \;=\; 1.89252 \pm 0.00018 \tag{2.21}$$

$$V_{10} \;=\; 2.53956 \pm 0.00034 \tag{2.22}$$

In general, the formula for the $2n$-point function contains $(2n)!/[2(n!)^2]$ terms [this takes into account the $\{\epsilon_j\} \leftrightarrow \{-\epsilon_j\}$ symmetry], and this grows asymptotically like

[9] Unfortunately, Kamieniarz and Blöte [81] reported only meager details of the fits that led to this extraordinarily precise estimate. That is a shame, as information on the presence or absence of particular correction-to-scaling terms could be of considerable theoretical interest.

4^n. Thus, in computing V_4 (resp. V_6, V_8, V_{10}) we had to include 3 (resp. 10, 35, 126) terms, and the computation of V_{12} would require handling 462 terms. Moreover, the numerator has to be integrated over a $(4n-2)$-dimensional torus. These facts make the high-precision numerical integration of V_{2n} extremely time-consuming as soon as n becomes moderately large.

Let us consider, finally, the dimensionless renormalized four-point coupling constant g_4 defined by

$$g_4 \;=\; -\frac{\bar{u}_4}{\chi^2 \xi^d} \;=\; -\frac{U_4}{(\xi/L)^d} \;, \tag{2.23}$$

where $\bar{u}_4$ is the connected four-point function at zero momentum, and more generally the dimensionless renormalized $2n$-point coupling constant g_{2n} defined by

$$g_{2n} \;=\; \frac{\chi^n \, \bar{\Gamma}_{2n}}{\xi^{(n-1)d}} \;, \tag{2.24}$$

where $\bar{\Gamma}_{2n}$ is the amputated one-particle-irreducible $2n$-point function at zero momentum. In the FSS limit $L \to \infty$, $\beta \to \beta_c$ with ξ/L fixed, g_{2n} becomes a nontrivial function of the FSS variable ξ/L,

$$g_{2n} \;=\; F_{g_{2n}}(\xi/L) \;. \tag{2.25}$$

(There is some evidence that F_{g_4} is a *decreasing* function of ξ/L.[10]) In particular, the massive and massless scaling limits

$$g^*_{2n} \;=\; \lim_{\beta \uparrow \beta_c} \lim_{L \to \infty} g_{2n}(\beta, L) \tag{2.26}$$

$$G^*_{2n} \;=\; \lim_{L \to \infty} \lim_{\beta \uparrow \beta_c} g_{2n}(\beta, L) \;=\; \lim_{L \to \infty} g_{2n}(\beta_c, L) \tag{2.27}$$

correspond to the two extreme cases $g^*_{2n} = F_{g_{2n}}(0)$, $G^*_{2n} = F_{g_{2n}}(x^\star)$. The best currently available estimates for the 2D Ising model are

$$g^*_4 \;=\; \begin{cases} 14.694 \pm 0.002 & \text{by high-temperature expansion [84, 28]} \\ 14.66 \pm 0.42 & \text{by } \epsilon\text{-expansion [28]} \\ 15.50 \pm 0.84 & \text{by } g\text{-expansion [85]} \\ 14.66 \pm 0.06 & \text{by expansion around } d = 0 \text{ [86, 87]} \\ 14.7 \pm 0.2 & \text{by Monte Carlo [31]} \end{cases} \tag{2.28}$$

$$G^*_4 \;=\; 2.239 \pm 0.007 \qquad \text{by Monte Carlo [31]} \tag{2.29}$$

[10] Baker and Kawashima [82] conjecture that $g_4(\beta, L)$ [resp. $\xi(\beta, L)$] is a decreasing [resp. increasing] function of β for each fixed $L < \infty$; these two facts, if true, would immediately imply that $F_{g_4}(\xi/L)$ is a decreasing function of its argument ξ/L. Numerical data for the 2D [41, 83] and three-dimensional [41, 82] Ising models clearly support the Baker–Kawashima conjecture.

$$g_6^* = \begin{cases} 794.1 \pm 0.6 & \text{by high-temperature expansion [27, 28, 29]} \\ 797 \pm 9 & \text{by } \epsilon\text{-expansion [28, 29]} \\ 792 \pm 40 & \text{by } g\text{-expansion with constrained } g_4^* \text{ [30]} \\ 691 \pm 29 & \text{by expansion around } d = 0 \text{ [86, 87]} \\ 850 \pm 25 & \text{by Monte Carlo [31]} \end{cases} \tag{2.30}$$

$$G_6^* = 29.34 \pm 0.20 \qquad \text{by Monte Carlo [31]} \tag{2.31}$$

$$g_8^* = \begin{cases} (82.5 \pm 0.6) \times 10^3 & \text{by high-temperature expansion [28, 29]} \\ (83.8 \pm 3.2) \times 10^3 & \text{by } \epsilon\text{-expansion [28, 29]} \\ (89 \pm 5) \times 10^3 & \text{by Monte Carlo [31]} \end{cases} \tag{2.32}$$

$$G_8^* = 947 \pm 10 \qquad \text{by Monte Carlo [31]} \tag{2.33}$$

$$g_{10}^* = \begin{cases} (12.8 \pm 0.7) \times 10^6 & \text{by high-temperature expansion [28, 29]} \\ (8.0 \pm 1.4) \times 10^6 & \text{by } \epsilon\text{-expansion [28, 29]} \end{cases} \tag{2.34}$$

Our own Monte Carlo data, reported in Section 4.3, combined with the theoretical value (2.14) for $x^\star$, improve (2.29)/(2.31)/(2.33) to $G_4^* = 2.23685 \pm 0.00016$, $G_6^* = 29.2602 \pm 0.0047$ and $G_8^* = 942.91 \pm 0.25$, respectively, and also give values for G_{10}^* through G_{20}^* [see (4.20) and the footnote following it]. From (2.14) and (2.17)–(2.22) we obtain the theoretical predictions

$$G_4^* = -\frac{U_4}{x^{\star 2}} = 2.2366587 \pm 0.0000057 \tag{2.35a}$$

$$G_6^* = -\frac{U_6 - 10U_4^2}{x^{\star 4}} = 29.25457 \pm 0.00015 \tag{2.35b}$$

$$G_8^* = -\frac{U_8 - 56U_4U_6 + 280U_4^3}{x^{\star 6}} = 942.6095 \pm 0.0072 \tag{2.35c}$$

$$G_{10}^* = -\frac{U_{10} - 120U_4U_8 - 126U_6^2 + 4620U_4^2U_6 - 15400U_4^4}{x^{\star 8}} = 56110.24 \pm 0.56 \tag{2.35d}$$

The error bars in (2.35) are obtained by carefully propagating the statistical errors from the V_{2n} [in which the errors are independent except for an extremely small effect arising from the value of the denominator (2.12)] to the U_{2n} (in which the errors are correlated) and thence to the G_{2n}^*.

3 Numerical Simulations

We consider the two-dimensional nearest-neighbor Ising model on a $L \times L$ square lattice with periodic boundary conditions, given by the Hamiltonian

$$\mathcal{H}_{\text{Ising}} = -\frac{\beta}{2} \sum_{\langle ij \rangle} \sigma_i \sigma_j \tag{3.1a}$$

$$= -\beta \sum_{\langle ij \rangle} \delta_{\sigma_i, \sigma_j} + \text{const} . \tag{3.1b}$$

Note that we use throughout this paper a non-standard normalization of β, which is motivated by considering the Ising model as a special case of the q-state Potts model; it differs by a factor of 2 from the usual Ising normalization. In our normalization, the critical point is at

$$\beta_c = \log(1 + \sqrt{2}) \approx 0.881373587 . \tag{3.2}$$

3.1 Observables to be measured

We have performed simulations of this system using the Swendsen-Wang algorithm [88, 89, 90]. In particular, we have measured the following basic observables:

- the energy density (i.e., the number of unsatisfied bonds)

$$\mathcal{E} \equiv \sum_{\langle xy \rangle} (1 - \delta_{\sigma_x, \sigma_y}) \tag{3.3}$$

- the bond occupation

$$\mathcal{N} \equiv \sum_{\langle xy \rangle} n_{xy} \tag{3.4}$$

- the nearest-neighbor connectivity (which is an energy-like observable [75])

$$\mathcal{E}' \equiv \sum_{\langle xy \rangle} \gamma_{xy} , \tag{3.5}$$

  where γ_{xy} equals 1 if both ends of the bond $\langle xy \rangle$ belong to the same cluster, and 0 otherwise. More generally, the connectivity γ_{ij} can be defined for an arbitrary pair i, j of sites:

$$\gamma_{ij}(\{n\}) = \begin{cases} 1 & \text{if } i \text{ is connected to } j \\ 0 & \text{if } i \text{ is not connected to } j \end{cases} \tag{3.6}$$

- the squared magnetization

$$\mathcal{M}^2 = \left(\sum_x \boldsymbol{\sigma}_x \right)^2 \tag{3.7a}$$

$$= \frac{q}{q-1} \sum_{\alpha=1}^{q} \left(\sum_x \delta_{\sigma_x, \alpha} \right)^2 - \frac{V^2}{q-1} \tag{3.7b}$$

where $\boldsymbol{\sigma}_x \equiv \mathbf{e}^{(\sigma_x)} \in \mathbf{R}^{q-1}$ is the Potts spin in the hypertetrahedral representation[11] and $V = L^2$ is the number of lattice sites

- powers of the squared magnetization

$$\mathcal{M}^{2n} \;=\; (\mathcal{M}^2)^n \tag{3.8}$$

- the square of the Fourier transform of the spin variable at the smallest allowed non-zero momentum

$$\mathcal{F} \;=\; \frac{1}{2}\left(\left|\sum_x \boldsymbol{\sigma}_x\, e^{2\pi i x_1/L}\right|^2 + \left|\sum_x \boldsymbol{\sigma}_x\, e^{2\pi i x_2/L}\right|^2\right) \tag{3.9a}$$

$$\;=\; \frac{q}{q-1} \times \frac{1}{2}\sum_{\alpha=1}^{q}\left(\left|\sum_x \delta_{\sigma_x,\alpha}\, e^{2\pi i x_1/L}\right|^2 + \left|\sum_x \delta_{\sigma_x,\alpha}\, e^{2\pi i x_2/L}\right|^2\right) \tag{3.9b}$$

where (x_1, x_2) are the Cartesian coordinates of point x. Note that $\mathcal{F}$ is normalized to be comparable to its zero-momentum analogue $\mathcal{M}^2$.

- the mean-square and mean-fourth-power size of the clusters

$$\mathcal{S}_2 \;=\; \sum_{\mathcal{C}} \#(\mathcal{C})^2 \tag{3.10}$$

$$\mathcal{S}_4 \;=\; \sum_{\mathcal{C}} \#(\mathcal{C})^4 \tag{3.11}$$

where the sum is over all the clusters $\mathcal{C}$ of activated bonds and $\#(\mathcal{C})$ is the number of sites in the cluster $\mathcal{C}$.

From these observables we compute the following expectation values:

- the energy density E per spin

$$E \;=\; \frac{1}{V}\langle \mathcal{E} \rangle \tag{3.12}$$

- the specific heat

$$C_H \;=\; \frac{1}{V}\mathrm{var}(\mathcal{E}) \equiv \frac{1}{V}\left[\langle \mathcal{E}^2 \rangle - \langle \mathcal{E} \rangle^2\right] \tag{3.13}$$

- the magnetic susceptibility

$$\chi \;=\; \frac{1}{V}\langle \mathcal{M}^2 \rangle \tag{3.14}$$

- the higher magnetization cumulants

$$\bar{u}_{2n} \;=\; \frac{1}{V}\langle \mathcal{M}^{2n} \rangle_{\mathrm{conn}} \tag{3.15}$$

[11] Let $\{\mathbf{e}^{(\alpha)}\}_{\alpha=1}^{q}$ be unit vectors in $\mathbf{R}^{q-1}$ satisfying $\mathbf{e}^{(\alpha)} \cdot \mathbf{e}^{(\beta)} = (q\delta^{\alpha\beta} - 1)/(q-1)$, and let $\boldsymbol{\sigma}_x \equiv \mathbf{e}^{(\sigma_x)}$. For $q = 2$ this means $\boldsymbol{\sigma}_x = \cos(\pi\sigma_x) = \pm 1$.

- the magnetization moment ratios

$$V_{2n} \;=\; \frac{\langle \mathcal{M}^{2n} \rangle}{\langle \mathcal{M}^2 \rangle^n} \tag{3.16}$$

- the correlation function at momentum $(2\pi/L, 0)$

$$F \;=\; \frac{1}{V} \langle \mathcal{F} \rangle \tag{3.17}$$

- the second-moment correlation length

$$\xi \;=\; \frac{1}{2\sin(\pi/L)} \left(\frac{\chi}{F} - 1 \right)^{1/2} \tag{3.18}$$

- the variant second-moment correlation length

$$\xi' \;=\; \frac{L}{2\pi} \left(\frac{\chi}{F} - 1 \right)^{1/2} \;, \tag{3.19}$$

  which differs from ξ only by correction-to-scaling terms of order L^{-2}

Remarks. 1. Using the Fortuin–Kasteleyn identities [91, 92, 93, 90], it is not difficult to show that

$$\langle \mathcal{N} \rangle \;=\; p(B - \langle \mathcal{E} \rangle) \tag{3.20}$$

$$\langle \mathcal{E} \rangle \;=\; \frac{q}{q-1} (B - \langle \mathcal{E}' \rangle) \tag{3.21}$$

$$\langle \mathcal{M}^2 \rangle \;=\; \langle \mathcal{S}_2 \rangle \tag{3.22}$$

$$\langle \mathcal{M}^4 \rangle \;=\; \frac{q+1}{q-1} \langle \mathcal{S}_2^2 \rangle - \frac{2}{q-1} \langle \mathcal{S}_4 \rangle \tag{3.23}$$

where $p = 1 - e^{-\beta}$ and $B = 2V$ is the number of bonds in the lattice. As a check on the correctness of our simulations, we have tested these identities to high precision, in the following way: Instead of comparing directly the left and right sides of each equation, which are strongly positively correlated in the Monte Carlo simulation, a more sensitive test is to define new observables corresponding to the differences (i.e., $\mathcal{N} - p(B - \mathcal{E})$ and so forth). Each such observable should have mean zero, and the error bars on the sample mean can be estimated using the standard error analysis outlined below. The comparison to zero yields the following χ^2 values:

$$\text{For (3.20):} \qquad \chi^2 = 10.23 \text{ (14 DF, level = 75\%)} \tag{3.24}$$

$$\text{For (3.21):} \qquad \chi^2 = 17.00 \text{ (14 DF, level = 26\%)} \tag{3.25}$$

$$\text{For (3.22):} \qquad \chi^2 = \;\; 9.93 \text{ (14 DF, level = 77\%)} \tag{3.26}$$

$$\text{For (3.23):} \qquad \chi^2 = \;\; 9.05 \text{ (14 DF, level = 83\%)} \tag{3.27}$$

Here DF means the number of degrees of freedom, and "level" means the confidence level of the fit (defined at the beginning of Section 4 below). The agreement is excellent.

2. We also compared our data for V_4 for $L = 4, 6, 8, 12, 16$ with the exact values computed by Kamieniarz and Blöte [81] using transfer-matrix methods. We get $\chi^2 = 5.14$ (5 DF, level = 40%), indicating good agreement.

For each observable $\mathcal{O}$ discussed above we have measured its autocorrelation functions in the Swendsen-Wang dynamics,

$$C_{\mathcal{O}\mathcal{O}}(t) \;=\; \langle \mathcal{O}_s \mathcal{O}_{s+t} \rangle - \langle \mathcal{O} \rangle^2 \tag{3.28}$$

$$\rho_{\mathcal{O}\mathcal{O}}(t) \;=\; \frac{C_{\mathcal{O}\mathcal{O}}(t)}{C_{\mathcal{O}\mathcal{O}}(0)} \tag{3.29}$$

where the expectations are taken in equilibrium. From these functions we have estimated the corresponding integrated autocorrelation time

$$\tau_{\mathrm{int},\mathcal{O}} \;=\; \frac{1}{2} \sum_{t=-\infty}^{\infty} \rho_{\mathcal{O}\mathcal{O}}(t) \tag{3.30a}$$

$$\;=\; \frac{1}{2} + \sum_{t=1}^{\infty} \rho_{\mathcal{O}\mathcal{O}}(t) \tag{3.30b}$$

by the methods of Ref. [94, Appendix C], using a self-consistent truncation window of width $6\tau_{\mathrm{int},\mathcal{O}}$. This autocorrelation time is needed to compute the correct error bar on the sample mean $\overline{\mathcal{O}}$.

Remarks. 1. The error bar of the second-moment correlation length is computed by considering the random variable

$$\mathcal{O}' \;=\; \frac{\mathcal{M}^2}{\mu_{\mathcal{M}^2}} - \frac{\mathcal{F}}{\mu_{\mathcal{F}}} \,, \tag{3.31}$$

which automatically has zero mean. Then,

$$\mathrm{var}(\widehat{\xi})^{1/2} \;=\; \frac{1}{4\sin(\pi/L)} \frac{\chi}{F} \left(\frac{\chi}{F} - 1 \right)^{-1/2} \mathrm{var}(\mathcal{O}')^{1/2} \,, \tag{3.32}$$

where $\widehat{\xi}$ denotes our Monte Carlo estimate of ξ. In practice, the values of $\mu_{\mathcal{M}^2}$ and $\mu_{\mathcal{F}}$ are replaced by their corresponding sample means (which should be computed first).

2. The error bar on the ratio V_{2n} is computed in a similar fashion:

$$\mathrm{var}(\widehat{V}_{2n})^{1/2} \;=\; \frac{\langle \mathcal{M}^{2n} \rangle}{\langle \mathcal{M}^2 \rangle^n} \mathrm{var}(\mathcal{O}''_{2n})^{1/2} \,, \tag{3.33}$$

where $\widehat{V}_{2n}$ denotes our Monte Carlo estimate of V_{2n}, and the observable $\mathcal{O}''_{2n}$ is defined as

$$\mathcal{O}''_{2n} \;=\; \frac{\mathcal{M}^{2n}}{\mu_{\mathcal{M}^{2n}}} - n \frac{\mathcal{M}^2}{\mu_{\mathcal{M}^2}} + n - 1 \tag{3.34}$$

and has mean zero. Again, the mean values $\mu_{\mathcal{M}^{2n}}$ and $\mu_{\mathcal{M}^2}$ are replaced in practice by their sample means.

3. As a further check on the correctness of our simulations, we have computed both sides of the identity

$$\rho_{\mathcal{N}\mathcal{N}}(1) \;=\; 1 - \frac{(1-p)(2-E)}{pC_H + (1-p)(2-E)} \tag{3.35}$$

proven in [95, equation 7] (see also [75]).[12] This is a highly nontrivial test, as it relates static quantities (energy and specific heat) to a dynamic quantity (autocorrelation function of the bond occupation at time lag 1). We have also checked with great accuracy the identities [75]

$$C_{\mathcal{E}\mathcal{E}}(t) \;=\; \frac{1}{p^2} C_{\mathcal{N}\mathcal{N}}(t+1) \tag{3.36}$$

$$\rho_{\mathcal{E}\mathcal{E}}(t) \;=\; \frac{\rho_{\mathcal{N}\mathcal{N}}(t+1)}{\rho_{\mathcal{N}\mathcal{N}}(1)} \tag{3.37}$$

$$C_{\mathcal{E}'\mathcal{E}'}(t) \;=\; \left(\frac{q}{q-1}\right)^2 C_{\mathcal{E}\mathcal{E}}(t+1) \tag{3.38}$$

$$\rho_{\mathcal{E}'\mathcal{E}'}(t) \;=\; \frac{\rho_{\mathcal{E}\mathcal{E}}(t+1)}{\rho_{\mathcal{E}\mathcal{E}}(1)} \tag{3.39}$$

3.2 Summary of the simulations

We have run our Monte Carlo program on lattices with L ranging from 4 to 512 (see Table 1). In all cases the initial configuration was random, and for $L \le 64$ (resp. $L \ge 96$) we discarded the first 5×10^4 (resp. 10^5) iterations to allow the system to reach equilibrium; this discard interval is in all cases greater than $10^4\, \tau_{\mathrm{int},\mathcal{E}}$.[13] The total number of iterations ranges from 2.15×10^6 ($L = 4$) to 8.2×10^6 ($L = 512$), and is selected to be approximately $10^6\, \tau_{\mathrm{int},\mathcal{E}}$. These statistics allow us to obtain a high accuracy in our estimates of the static and dynamic quantities (error $\lesssim 0.17\%$ and $\lesssim 0.51\%$, respectively). The static data are displayed in Table 1 (χ, F, ξ) and Table 2 (the ratios V_{2n}). The dynamic data will be reported elsewhere.

The CPU time required by our program is approximately 6.3 L^2 μs per iteration on a Linux Pentium machine running at 166 MHz. The total CPU time used in the project was approximately 7.5 months on this machine.

[12] Please note that [95] used a definition of energy that is slightly different from the one used here: $E(\text{Ref. [95]}) = (1/V)\langle \sum_{\langle xy \rangle} \delta_{\sigma_x,\sigma_y} \rangle = 2 - E$.

[13] Such a discard interval might seem to be much larger than necessary: $10^2 \tau_{\mathrm{int}}$ would usually be more than enough. However, there is always the danger that the longest autocorrelation time in the system may be much larger than the longest autocorrelation time that one has *measured*, because one has failed to measure an observable having sufficiently strong overlap with the slowest mode. As an undoubtedly overly conservative precaution against the possible (but unlikely) existence of such a (vastly) slower mode, we decided to discard up to 2% of the entire run. This discard amounts to reducing the accuracy on our final estimates by a mere 1%.

We have improved the precision of our analysis of the correlation length ξ by supplementing our own Monte Carlo data with comparable data from Ballesteros *et al.* [96]. They performed single-cluster [97] simulations of the 2D site-diluted Ising model at various concentrations p. Their data for $\mathsf{p} = 1$ (i.e., the usual Ising model) correspond to anywhere from 4×10^5 to 7×10^5 statistically independent measurements at each lattice size from $L = 12$ to $L = 512$ (see Table 3). The statistical independence of two consecutive measurements was achieved by allowing 100 single-cluster moves between them. Their error bars are slightly larger than ours. As a matter of fact, their error bars $\sigma'(\xi)$ and our error bars $\sigma(\xi)$ satisfy approximately the relation

$$\frac{\sigma(\xi)}{\sigma'(\xi)} \;=\; \sqrt{\frac{2\tau_{\mathrm{int},\mathcal{O}'}N'}{N}} \;, \tag{3.40}$$

where N (resp. N') is the number of measurements of our (resp. their) work, and $\mathcal{O}'$ is the observable (3.31) we used to compute the correct correlation-length error bar. This supports the belief that their measurements are indeed essentially independent and that their error bars are correctly computed. Comparison of their raw data to ours at the eleven overlapping L values yields $\chi^2 = 10.28$ (11 DF, level = 51%). The two data sets are therefore compatible. The corresponding merged data are shown in Table 4.

4 Data Analysis

For each quantity $\mathcal{O}$, we carry out a variety of fits using the standard weighted least-squares method. As a precaution against corrections to scaling, we impose a lower cutoff $L \geq L_{min}$ on the data points admitted in the fit, and we study systematically the effects of varying L_{min} on the estimated parameters and on the χ^2 value. In general, our preferred fit corresponds to the smallest L_{min} for which the goodness of fit is reasonable (e.g., the confidence level[14] is $\gtrsim$ 10–20%) and for which subsequent increases in L_{min} do not cause the χ^2 to drop vastly more than one unit per degree of freedom (DF).

4.1 Corrections to scaling

In the data analysis we should take into account the effect of corrections to scaling in order to get reliable estimates of the physical quantities. In particular, the value at criticality of any observable $O(L)$ is typically given for large L by

$$O(L) = AL^{p_O}\left(1 + A'L^{-\Delta} + \cdots\right) \tag{4.1}$$

[14] "Confidence level" is the probability that χ^2 would exceed the observed value, assuming that the underlying statistical model is correct. An unusually low confidence level (e.g., less than 5%) thus suggests that the underlying statistical model is *incorrect* — the most likely cause of which would be corrections to scaling.

where p_O is the critical exponent associated to the observable O, Δ is the leading correction-to-scaling exponent, and the dots indicate higher-order corrections.

In finite-size-scaling (FSS) theory [98] for systems with periodic boundary conditions, three simplifying assumptions have frequently been made:

(a) The regular part of the free energy, $f_{\rm reg}$, is independent of L [98] (except possibly for terms that are exponentially small in L).

(b) The relations connecting the nonlinear scaling fields g_t and g_h to the conventional thermodynamic parameters $t \equiv \beta_c - \beta$ and h are independent of L [99].

(c) The scaling field g_L associated to the lattice size equals L^{-1} exactly, with no corrections L^{-2}, L^{-3}, ... [98].

Moreover, in the nearest-neighbor spin-1/2 2D Ising model, it has further been assumed that

(d) There are no irrelevant operators [100, 101].

This latter assumption has been confirmed numerically (in the infinite-volume theory) through order t^3, at least as regards the bulk behavior of the susceptibility [101]. However, both numerical [102, 103] and theoretical [104] evidence has recently emerged suggesting that irrelevant operators *do* contribute to the susceptibility at order t^4.

The absence of irrelevant operators implies that the corrections to scaling in this model are due to the smooth but in general nonlinear connection between the conventional thermodynamic parameters t and h and the renormalization-group nonlinear scaling fields [105, 106, 100, 101]. Starting from the FSS Ansatz for the Ising-model free energy and using the above assumptions, it is possible to obtain a FSS expression for the usual observables at criticality as functions of the lattice size L [107]. In particular, the leading correction term in the expansion of the susceptibility is the L-independent term coming from the regular part of the free energy. This implies that for this observable

$$\Delta \;=\; \frac{7}{4} \;. \tag{4.2}$$

The same result is plausible for the observable F defined in (3.17); thus, we expect $\Delta = 7/4$ for the second-moment correlation lengths ξ and ξ' and the corresponding amplitude $x^\star$. The expansion for the magnetization cumulant $\bar{u}_{2n}$ gives an exponent $\Delta = 1 + \gamma/\nu = 11/4$ (perhaps with a multiplicative logarithmic correction). Thus, we expect that the ratios V_{2n} also have a correction-to-scaling exponent given by (4.2) [due to the power of the susceptibility appearing in its definition (1.1)]. For a more detailed theoretical and numerical analysis of the corrections to scaling in this model, see [107].

4.2 Second-moment correlation length

The second-moment correlation length ξ and its variant ξ' [cf. (3.18)/(3.19)] are expected to behave as

$$\left\{ \begin{matrix} \xi \\ \xi' \end{matrix} \right\} \;=\; L^p \left[x^\star + A L^{-\Delta} + \cdots \right] \tag{4.3}$$

with $p = 1$. We can estimate p by ignoring correction-to-scaling terms and performing a simple power-law fit. We get

$$\text{For } \xi\text{:} \quad p = 0.99974 \pm 0.00036 \qquad (L_{min} = 32,\ \chi^2 = 1.48,\ 6 \text{ DF, level} = 96\%) \tag{4.4}$$

$$\text{For } \xi'\text{:} \quad p = 1.00018 \pm 0.00036 \qquad (L_{min} = 32,\ \chi^2 = 1.37,\ 6 \text{ DF, level} = 97\%) \tag{4.5}$$

The agreement with the theoretical prediction is excellent.

The value of the constant $x^\star$ can be estimated most simply by fitting the ratio ξ/L or ξ'/L to a constant, ignoring corrections to scaling. We get

$$\text{For } \xi\text{:} \quad x^\star = 0.90577 \pm 0.00028 \qquad (L_{min} = 32,\ \chi^2 = 2.02,\ 7 \text{ DF, level} = 96\%) \tag{4.6}$$

$$\text{For } \xi'\text{:} \quad x^\star = 0.90557 \pm 0.00026 \qquad (L_{min} = 16,\ \chi^2 = 2.73,\ 9 \text{ DF, level} = 97\%) \tag{4.7}$$

The estimate based on ξ lies 2.6 standard deviations away from the value $x^\star \approx 0.90505$ predicted by CFT [cf. (2.14)]. The estimate based on ξ' is slightly better: it lies two standard deviations away from the theoretical prediction, and works also for smaller L_{min}. Indeed, the corrections to scaling in ξ'/L are negligible (compared to our statistical error) already for $L \geq 16$ (see the last column of Table 4).[15] This fact makes it almost hopeless to study corrections to FSS in ξ'.

If we fit ξ to (4.3), keeping the first correction-to-scaling term and trying to estimate simultaneously the three parameters $x^\star$, A and Δ, a good fit is obtained for $L_{min} = 8$:

$$x^\star \;=\; 0.90546 \pm 0.00033 \tag{4.8a}$$

$$A \;=\; 0.75 \pm 0.30 \tag{4.8b}$$

$$\Delta \;=\; 1.76 \pm 0.18 \tag{4.8c}$$

with $\chi^2 = 2.97$ (9 DF, level = 97%). The value of $x^\star$ is again two standard deviations away from the theoretical prediction (2.14). The estimate of Δ is very close to 7/4, and is only 1.4 standard deviations away from 2; but perhaps this estimate ought not be taken too seriously, as the correction-to-scaling amplitude is only 2.5

[15] Table 4 is based on merging our data with that of Ballesteros *et al.* [96]; but virtually identical results are obtained using our data alone.

standard deviations away from zero (a deviation that is, moreover, comparable to the discrepancy in $x^\star$). The analogous fit for ξ' is even more hopeless (the amplitude A is compatible with zero within 0.7 standard deviations), so we omit the details. This correction-to-scaling exponent $\Delta \approx 2$ can be understood as arising simply from the ratio $\xi/\xi' \equiv [(L/\pi)\sin(\pi/L)]^{-1} = 1 + (\pi^2/6)L^{-2} + \ldots$. Indeed, if we fit the data to the Ansatz $\xi/L = x^\star + AL^{-2}$ we get for $L_{min} = 8$:

$$x^\star = 0.90569 \pm 0.00027 \tag{4.9a}$$

$$A = 1.269 \pm 0.064 \tag{4.9b}$$

with $\chi^2 = 4.56$ (10 DF, level = 92%). Then, $A/x^\star \approx 1.40$, which is not far from $\pi^2/6 \approx 1.64$.

We can improve the precision of our numerical estimates by using the merged data of Table 4 (our data plus that of Ballesteros *et al.* [96]). The simple power-law fit yields

$$\text{For } \xi\text{:} \quad p = 1.00047 \pm 0.00033 \qquad (L_{min} = 48,\ \chi^2 = 0.86,\ 5 \text{ DF, level} = 97\%) \tag{4.10}$$

$$\text{For } \xi'\text{:} \quad p = 1.00074 \pm 0.00033 \qquad (L_{min} = 48,\ \chi^2 = 0.82,\ 5 \text{ DF, level} = 98\%) \tag{4.11}$$

The fits to a constant give

$$\text{For } \xi\text{:} \quad x^\star = 0.90565 \pm 0.00023 \qquad (L_{min} = 48,\ \chi^2 = 2.92,\ 6 \text{ DF, level} = 82\%) \tag{4.12}$$

$$\text{For } \xi'\text{:} \quad x^\star = 0.90555 \pm 0.00020 \qquad (L_{min} = 16,\ \chi^2 = 6.99,\ 9 \text{ DF, level} = 64\%) \tag{4.13}$$

The three-parameter fit $\xi/L = x^\star + AL^{-\Delta}$ is good for $L_{min} = 8$:

$$x^\star = 0.90552 \pm 0.00026 \tag{4.14a}$$

$$A = 0.86 \pm 0.29 \tag{4.14b}$$

$$\Delta = 1.82 \pm 0.15 \tag{4.14c}$$

with $\chi^2 = 7.57$ (9 DF, level = 58%). The analogous fit with ξ' yields a correction-to-scaling amplitude compatible with zero within errors.

In conclusion, one can extract accurate estimates of the critical exponent p and the amplitude $x^\star$ using our Monte Carlo data; the results agree with the theoretical prediction (2.14) within two standard deviations. However, it is very difficult to estimate from our numerical data the correction-to-scaling exponent (or the corresponding amplitude). Indeed, for ξ' the corrections to scaling are negligible (compared to our statistical error) for $L \geq 16$.

4.3 Magnetization moment ratios

If we study the magnetization distribution $\rho(\mathcal{M})$ as $L \to \infty$ at fixed β, we expect three distinct behaviors depending on the value of β:

(a) At $\beta < \beta_c$, we are in the high-temperature regime, where correlations decay exponentially. A variant of the central limit theorem [108] guarantees that the finite-L distributions will converge, after rescaling by the factor $\sqrt{V\chi}$, to a Gaussian distribution of mean zero and unit variance.[16]

(b) At $\beta > \beta_c$ we are in the low-temperature regime, and the finite-L distributions should converge, after rescaling by the factor VM_0 (where M_0 is the spontaneous magnetization), to the sum of two delta functions. There are Gaussian fluctuations around these two delta functions, but their width is much smaller, namely $\sqrt{V\chi_0}$, where χ_0 is the susceptibility in a pure phase.

(c) At $\beta = \beta_c$ [or more generally, at fixed value of the FSS variable $L^{1/\nu}(\beta - \beta_c)$], the finite-$L$ distributions will converge, after rescaling by the factor $\sqrt{V\chi}$, to some non-Gaussian distribution characteristic of the critical Ising model in a finite box. This distribution is not, to our knowledge, known exactly.

We have computed the magnetization histograms at $\beta = \beta_c$ for $L = 4, \ldots, 512$. The sequence of histograms is expected to converge to a limiting distribution when we normalize the magnetization by $\sqrt{V\chi}$ and normalize the height of the bins so that the area enclosed by the histogram is 1. For $L \gtrsim 64$ the histograms converge well to a limiting histogram (Figure 1). For $L \lesssim 48$ small corrections to scaling are observed: the peaks of the histogram are slightly taller than in the limiting histogram The limiting distribution is symmetric and very strongly two-peaked (with maxima at $\mathcal{M}/\sqrt{V\chi} \approx \pm 1.11$); clearly the 2D Ising model at criticality in a finite symmetric torus is very far from Gaussian (e.g., we will find V_4 much closer to 1 than to 3).

In order to characterize quantitatively this limiting distribution, we have measured its moments $\langle \mathcal{M}^{2n} \rangle$ for $n = 1, \ldots, 10$ and have computed the corresponding ratios $V_{2n} \equiv \langle \mathcal{M}^{2n} \rangle / \langle \mathcal{M}^2 \rangle^n$. We expect a behavior

$$V_{2n} \;=\; V_{2n}^{\infty} + B_{2n} L^{-\Delta} + \cdots \;. \tag{4.15}$$

For each n, we have fitted our numerical data (Table 2) in two ways: a one-parameter fit to a constant $V_{2n} = V_{2n}^{\infty}$ (fits marked with a C on the second column of Table 5) and a three-parameter fit to $V_{2n} = V_{2n}^{\infty} + B_{2n} L^{-\Delta}$ (fits marked P in Table 5).

As expected, the estimates of V_{2n}^{∞} lie in-between the values associated to a Gaussian distribution (1.5) and those associated to a two-delta-function distribution (1.6). However, they are much closer to the latter values, reflecting the strongly two-peaked shape of the magnetization distribution.

The fits to a constant are excellent for $L_{min} \gtrsim 32$–64; for $2n = 4, 6, 8, 10$ the estimates of V_{2n}^{∞} agree with the theoretical predictions within about 2.5 standard deviations. The three-parameter fits are excellent already for $L_{min} = 8$: the correction-to-

[16] Previously this had been proven for finite subvolumes of an infinite system [109, 110], by a technique using the FKG inequalities. It has recently been proven by Newman [108] also for finite systems with periodic or free boundary conditions, by a different (but simple and elegant) method using the GKS, GHS and Simon-Lieb inequalities. We thank Professor Newman for communicating to us this unpublished result, which we hope he will someday publish.

scaling amplitude B_{2n} grows in magnitude with n, while the values of the correction-to-scaling exponent Δ are quite stable and are consistent with the theoretical prediction $\Delta = \gamma/\nu = 7/4$ [cf. (4.2)] within two standard deviations.

Let us now look more closely at V_4. With the three-parameter fit, we obtain for $L_{min} = 8$:

$$V_4^\infty = 1.16777 \pm 0.00013 \tag{4.16a}$$
$$\Delta = 2.01 \pm 0.22 \tag{4.16b}$$
$$B_4 = -0.48 \pm 0.23 \tag{4.16c}$$

with $\chi^2 = 1.53$ (9 DF, level = 100%). The estimate of V_4^∞ is about one standard deviation away from the theoretical prediction $V_4^\infty \approx 1.16792$ [cf. (2.17)]. The estimate of Δ is reasonably close to $\Delta = 7/4$; but since the estimated correction amplitude B_4 is only 2 standard deviations away from zero, this estimate of Δ should perhaps not be taken too seriously.

Similarly, the estimates

$$V_6^\infty = 1.45517 \pm 0.00037 \tag{4.17}$$
$$V_8^\infty = 1.89163 \pm 0.00079 \tag{4.18}$$
$$V_{10}^\infty = 2.5377 \pm 0.0015 \tag{4.19}$$

from the three-parameter fit are compatible with the predicted exact values (2.20)/(2.21)/(2.22) within 1.5, 1.3 and 1.2 standard deviations, respectively. The estimates of the exponent Δ (1.90±0.16, 1.83±0.13 and 1.78±0.11, respectively) are compatible with 7/4.

The values of the first nine dimensionless renormalized $2n$-point coupling constants at criticality on a symmetric torus can be obtained from the results contained in Table 5:

$$G_4^* = 2.23685 \pm 0.00016 \tag{4.20a}$$
$$G_6^* = 29.2602 \pm 0.0047 \tag{4.20b}$$
$$G_8^* = 942.91 \pm 0.25 \tag{4.20c}$$
$$G_{10}^* = (5.6135 \pm 0.0021) \times 10^4 \tag{4.20d}$$
$$G_{12}^* = (5.3281 \pm 0.0026) \times 10^6 \tag{4.20e}$$
$$G_{14}^* = (7.3681 \pm 0.0046) \times 10^8 \tag{4.20f}$$
$$G_{16}^* = (1.3969 \pm 0.0010) \times 10^{11} \tag{4.20g}$$
$$G_{18}^* = (3.4746 \pm 0.0031) \times 10^{13} \tag{4.20h}$$
$$G_{20}^* = (1.0969 \pm 0.0011) \times 10^{16} \tag{4.20i}$$

The central values in (4.20), which are intended as our "best estimates", are computed using the *theoretical* value (2.14) for $x^\star$.[17] The error bars quoted in (4.20) are upper

[17] A "pure" Monte Carlo value, using the estimate (4.14a) for $x^\star$ in place of (2.14), can be obtained by dividing the central value in (4.20) by 1.005206^{2n-2} and adding $(2n-2) \times 0.000287$ to the

bounds computed using the triangle inequality, since we did not bother to compute the covariances among our Monte Carlo estimates of V_{2n}^∞. Of course, for $G_4^*, G_6^*, G_8^*, G_{10}^*$ the estimates (4.20a–d) are supplanted by the much more precise theoretical values (2.35a–d).

In summary, we have been able to estimate the limiting values V_{2n}^∞ with great accuracy; and in the cases where the exact values are known, our numerical estimates agree with the theoretical predictions within less than two standard deviations. Our numerical estimates for Δ are compatible (within less than two standard deviations) with $\Delta = 7/4$.

5 Conclusions

We have computed, using results from conformal field theory (CFT), the exact (except for numerical integration) values of five universal amplitude ratios characterizing the 2D Ising model at criticality on a symmetric torus: the correlation-length ratio $x^\star$ and the magnetization moment ratios V_4, V_6, V_8 and V_{10}. All except for V_4 are new, and we have improved previous CFT determinations of V_4 by three orders of magnitude (reaching precision similar to that obtained by transfer-matrix approaches). As a corollary, we have computed the exact values G_4^*, G_6^*, G_8^* and G_{10}^* of the first four dimensionless renormalized $2n$-point coupling constants at criticality on a symmetric torus.

We have checked all these theoretical predictions by means of a high-precision Monte Carlo simulation. Using finite-size-scaling (FSS) techniques, we have tried to determine the leading term as well as the correction-to-scaling terms. We confirm to high precision the theoretically predicted universal amplitude ratios $x^\star$, V_4, V_6, V_8 and V_{10} (error bars $\lesssim 0.06\%$).

The determination of the leading correction-to-scaling exponent Δ has proved to be difficult. For the modified correlation length ξ', the corrections to FSS are so weak that they are essentially invisible for $L \geq 16$; and no reliable conclusions can be obtained from our data for $L = 4, 6, 8, 12$. For the standard correlation length ξ, the leading correction to scaling might be $\Delta = 7/4$, or it might be $\Delta = 2$ arising from $\xi/\xi' \equiv [(L/\pi)\sin(\pi/L)]^{-1} = 1 + (\pi^2/6)L^{-2} + \ldots$. For the magnetization moment ratios V_{2n} we obtain stable results compatible with $\Delta = 7/4$ within two standard deviations, in agreement with the theoretical prediction (4.2).

It would be interesting to extend the analytic computation of $x^\star$ to other two-dimensional models, in particular those that can be mapped onto Gaussian models via height representations (see e.g. [111, 112, 78]). This work is currently in progress [113].

---

fractional error bar. Note that the *dominant* contribution to the error bar on G_{2n}^* would then come from the uncertainty on $x^\star$: for example, we would have $G_4^* = 2.2345 \pm 0.0014$, $G_6^* = 29.199 \pm 0.038$, $G_8^* = 939.97 \pm 1.87$, etc. in place of (4.20).

A Computation of spin-correlator integrals

The computation of $x^\star = \lim_{L\to\infty} \xi/L$ involves computing numerically the integrals

$$I_1 = \int d^2z \, \frac{\sum_{\nu=1}^{4} |\theta_\nu(z/2)|}{|\theta_1(z)|^{1/4}} \tag{A.1}$$

$$I_2 = \int d^2z \, \frac{\sum_{\nu=1}^{4} |\theta_\nu(z/2)|}{|\theta_1(z)|^{1/4}} \, \cos(2\pi x_1) \tag{A.2}$$

where $z = x_1 + i x_2$ and $\int d^2z = \int_0^1 \int_0^1 dx_1 \, dx_2$.

Let us consider here I_1, as I_2 can be done in a similar fashion. Using the symmetry properties of the θ-functions and their absolute values (see Appendix B), we reduce the integral to

$$I_1 = 4 \int_0^{1/2} \int_0^{1/2} dx_1 \, dx_2 \, \frac{\sum_{\nu=1}^{4} |\theta_\nu(z/2)|}{|\theta_1(z)|^{1/4}} \; . \tag{A.3}$$

The integrand contains two pieces: One (coming from $\nu = 1$) is finite at $z = 0$ and its integral can be performed safely by standard deterministic numerical-integration techniques (e.g. MATHEMATICA's `NIntegrate`), yielding

$$I_{1,1} \equiv 4 \int_0^{1/2} \int_0^{1/2} dx_1 \, dx_2 \, \frac{|\theta_1(z/2)|}{|\theta_1(z)|^{1/4}} = 0.5234826517 \pm 0.0000000001 \tag{A.4}$$

The other piece (coming from $\nu = 2, 3, 4$) diverges at $z = 0$ like $|\theta_1(z)|^{-1/4} \sim |z|^{-1/4}$. This singularity makes numerical integration a bit tricky. Since $\theta_1'(0) = 2\pi\eta^3$ [see (B.13)], the simple function

$$H(z) = 4 \, \frac{\sum_{\nu=2}^{4} |\theta_\nu(0)|}{|2\pi\eta^3 z|^{1/4}} \tag{A.5}$$

has exactly the same divergent behavior at $z = 0$. The integral of this function is given by

$$\begin{aligned}
4 \int_0^{1/2} \int_0^{1/2} dx_1 \, dx_2 \, H(z) &= 4 \, \frac{\sum_{\nu=2}^{4} |\theta_\nu(0)|}{(2\pi\eta^3)^{1/4}} \int_0^{1/2} \int_0^{1/2} dx_1 \, dx_2 \frac{1}{(x_1^2 + x_2^2)^{1/8}} \\
&= 8 \, \frac{\sum_{\nu=2}^{4} |\theta_\nu(0)|}{(2\pi\eta^3)^{1/4}} \int_0^{\pi/4} d\psi \int_0^{1/(2\cos\psi)} dr \; r^{3/4} \\
&= \frac{8 \, 2^{1/4}}{7} \frac{\sum_{\nu=2}^{4} |\theta_\nu(0)|}{(2\pi\eta^3)^{1/4}} \int_0^{\pi/4} (\cos\psi)^{-7/4} \, d\psi \\
&\approx 2.95015472419465
\end{aligned} \tag{A.6}$$

Though we were unable to perform exactly the final angular integral, the integrand $\cos^{-7/4}\psi$ is regular on the interval $[0, \pi/4]$ and so the integral can be performed by standard numerical-integration techniques.

Finally, we have to integrate the function

$$4 \, \frac{\sum_{\nu=2}^{4} |\theta_\nu(z/2)|}{|\theta_1(z)|^{1/4}} \; - \; H(z) \; . \tag{A.7}$$

This function does not diverge at $z = 0$ (or at any other point in the integration domain), so its integral can again be performed using standard techniques. This last integral is $0.007973883019 \pm 0.000000000001$, so the final result is

$$I_1 \;=\; 3.4816112589 \pm 0.0000000001 \; . \tag{A.8}$$

The second integral I_2 can be performed in the same way [and using the same auxiliary function $H(z)$]. The final result is

$$I_2 \;=\; 0.1044359092 \pm 0.0000000001 \; . \tag{A.9}$$

B Theta Functions

We use the following definitions for the Jacobi θ-functions [114, 115]:

$$\theta_1(z,\tau) \;\equiv\; -i \sum_{n=-\infty}^{\infty} (-1)^n y^{n+\frac{1}{2}} q^{\frac{1}{2}\left(n+\frac{1}{2}\right)^2} \tag{B.1a}$$

$$\;=\; 2 \sum_{n=0}^{\infty} (-1)^n q^{\frac{1}{2}\left(n+\frac{1}{2}\right)^2} \sin\left(2\pi \left(n+\frac{1}{2}\right) z\right) \tag{B.1b}$$

$$\theta_2(z,\tau) \;\equiv\; \sum_{n=-\infty}^{\infty} y^{n+\frac{1}{2}} q^{\frac{1}{2}\left(n+\frac{1}{2}\right)^2} \tag{B.2a}$$

$$\;=\; 2 \sum_{n=0}^{\infty} q^{\frac{1}{2}\left(n+\frac{1}{2}\right)^2} \cos\left(2\pi \left(n+\frac{1}{2}\right) z\right) \tag{B.2b}$$

$$\theta_3(z,\tau) \;\equiv\; \sum_{n=-\infty}^{\infty} y^n q^{\frac{1}{2}n^2} \tag{B.3a}$$

$$\;=\; 1 + 2 \sum_{n=1}^{\infty} q^{\frac{1}{2}n^2} \cos(2\pi n z) \tag{B.3b}$$

$$\theta_4(z,\tau) \;\equiv\; \sum_{n=-\infty}^{\infty} (-1)^n y^n q^{\frac{1}{2}n^2} \tag{B.4a}$$

$$\;=\; 1 + 2 \sum_{n=1}^{\infty} (-1)^n q^{\frac{1}{2}n^2} \cos(2\pi n z) \tag{B.4b}$$

where

$$q = e^{2\pi i\tau} \qquad \text{with } |q|<1 \tag{B.5a}$$
$$y = e^{2\pi iz} \tag{B.5b}$$

We sometimes omit the argument τ when its value is clear from the context; in particular, in the present paper we have usually $\tau = i$. A prime on θ_ν indicates the derivative with respect to z.

The θ-functions satisfy certain symmetry properties

$$\theta_1(z\pm 1) = -\theta_1(z) \tag{B.6a}$$
$$\theta_2(z\pm 1) = -\theta_2(z) \tag{B.6b}$$
$$\theta_3(z\pm 1) = \theta_3(z) \tag{B.6c}$$
$$\theta_4(z\pm 1) = \theta_4(z) \tag{B.6d}$$

$$\theta_1\left(z\pm\frac{1}{2}\right) = \pm\theta_2(z) \tag{B.7a}$$
$$\theta_2\left(z\pm\frac{1}{2}\right) = \mp\theta_1(z) \tag{B.7b}$$
$$\theta_3\left(z\pm\frac{1}{2}\right) = \theta_4(z) \tag{B.7c}$$
$$\theta_4\left(z\pm\frac{1}{2}\right) = \theta_3(z) \tag{B.7d}$$

$$\theta_1(z\pm\tau,\tau) = -y^{\mp1}q^{-1/2}\theta_1(z,\tau) \tag{B.8a}$$
$$\theta_2(z\pm\tau,\tau) = y^{\mp1}q^{-1/2}\theta_2(z,\tau) \tag{B.8b}$$
$$\theta_3(z\pm\tau,\tau) = y^{\mp1}q^{-1/2}\theta_3(z,\tau) \tag{B.8c}$$
$$\theta_4(z\pm\tau,\tau) = -y^{\mp1}q^{-1/2}\theta_4(z,\tau) \tag{B.8d}$$

$$\theta_1\left(z\pm\frac{\tau}{2},\tau\right) = \pm iy^{\mp1/2}q^{-1/8}\theta_4(z,\tau) \tag{B.9a}$$
$$\theta_2\left(z\pm\frac{\tau}{2},\tau\right) = y^{\mp1/2}q^{-1/8}\theta_3(z,\tau) \tag{B.9b}$$
$$\theta_3\left(z\pm\frac{\tau}{2},\tau\right) = y^{\mp1/2}q^{-1/8}\theta_2(z,\tau) \tag{B.9c}$$
$$\theta_4\left(z\pm\frac{\tau}{2},\tau\right) = \pm iy^{\mp1/2}q^{-1/8}\theta_1(z,\tau) \tag{B.9d}$$

Finally, it is worth noticing that the modulus of a θ-function satisfies the relation

$$|\theta_\nu(\pm x_1 \pm ix_2)| = |\theta_\nu(x_1+ix_2)| \tag{B.10}$$

for x_1, x_2 real and $0 \le q < 1$.

The Dedekind η-function is defined as

$$\eta(\tau) = q^{1/24} \prod_{n=1}^{\infty} (1 - q^n) \tag{B.11}$$

and it satisfies the relations

$$\theta_2(0,\tau)\theta_3(0,\tau)\theta_4(0,\tau) = 2\eta(\tau)^3 \tag{B.12}$$

$$\theta_1'(0,\tau) = 2\pi\eta(\tau)^3 \tag{B.13}$$

Acknowledgments

We wish to thank Juan Jesús Ruiz-Lorenzo for communicating to us his unpublished data; Chuck Newman for communicating to us his unpublished proof of a central limit theorem for periodic boxes; Sergio Caracciolo, Michael Fisher and Andrea Pelissetto for discussions; and Jae-Kwon Kim, Vladimir Privman and Hubert Saleur for correspondence. Finally, we wish to thank Carlos Naón, Anastasios Petkou, Andrei Smilga and Aleksandr Sokolov, who wrote to us after the first version of this paper was distributed in preprint form, for pointing out relevant bibliography that we had overlooked.

The authors' research was supported in part by U.S. National Science Foundation grants PHY-9520978 and PHY-9900769 (A.D.S.) and CICyT (Spain) grants PB95-0797 and AEN97-1680 (J.S.).

References

[1] C. Domb, *The Critical Point: A Historical Introduction to the Modern Theory of Critical Phenomena* (Taylor & Francis, London, 1996).

[2] V. Privman, P.C. Hohenberg and A. Aharony, in *Phase Transitions and Critical Phenomena*, Vol. 14, ed. C. Domb and J.L. Lebowitz (Academic Press, London–San Diego, 1991).

[3] B. Nienhuis, in *Phase Transitions and Critical Phenomena*, vol. 11, edited by C. Domb and J.L. Lebowitz (Academic Press, London, 1987).

[4] J.L. Cardy, in *Phase Transitions and Critical Phenomena*, vol. 11, edited by C. Domb and J.L. Lebowitz (Academic Press, London, 1987).

[5] C. Itzykson, H. Saleur and J.-B. Zuber, eds., *Conformal Invariance and Applications to Statistical Mechanics* (World Scientific, Singapore, 1988).

[6] P. Di Francesco, P. Mathieu and D. Sénéchal, *Conformal Field Theory* (Springer-Verlag, New York, 1997).

[7] J. Zinn-Justin, *Quantum Field Theory and Critical Phenomena*, 2nd edition (Clarendon Press, Oxford, 1993).

[8] R. Guida and J. Zinn-Justin, J. Phys. A **31**, 8103 (1998), cond-mat/9803240.

[9] G. Bhanot, M. Creutz and J. Lacki, Phys. Rev. Lett. **69**, 1841 (1992), hep-lat/9206020.

[10] J. Adler, C. Holm and W. Janke, Physica A **201**, 581 (1993), hep-lat/9305005.

[11] A.J. Guttmann and I.G. Enting, J. Phys. A **26**, 807 (1993), hep-lat/9212032.

[12] A.J. Guttmann and I.G. Enting, J. Phys. A **27**, 5801 (1994), hep-lat/9312083.

[13] H. Arisue and K. Tabata, Nucl. Phys. B **435**, 555 (1995), hep-lat/9407023.

[14] P. Butera and M. Comi, Phys. Rev. E **55**, 6391 (1997), hep-lat/9703017.

[15] P. Butera and M. Comi, Phys. Rev. B **56**, 8212 (1997), hep-lat/9703018.

[16] P. Butera and M. Comi, Phys. Rev. B **60**, 6749 (1999), hep-lat/9903010.

[17] C. Holm and W. Janke, Phys, Rev. B **48**, 936 (1993), hep-lat/9301002.

[18] A.P. Gottlob and M. Hasenbusch, Physica A **201**, 593 (1993), cond-mat/9305020.

[19] B. Li, N. Madras and A.D. Sokal, J. Stat. Phys. **80**, 661 (1995), hep-lat/9409003.

[20] H.W.J. Blöte, E. Liujten and J.R. Heringa, J. Phys. A **28**, 6289 (1995), cond-mat/9509016.

[21] M.P. Nightingale and H.W.J. Blöte, Phys. Rev. B **54**, 1001 (1996), cond-mat/9602089.

[22] H.W.J. Blöte, J.R. Heringa, A. Hoogland, E.W. Meyer and T.S. Smit, Phys. Rev. Lett. **76**, 2613 (1996), cond-mat/9602020.

[23] S. Caracciolo, M.S. Causo and A. Pelissetto, Phys. Rev. E **57**, 1215 (1998), cond-mat/9703250.

[24] H.G. Ballesteros, L.A. Fernández, V. Martín-Mayor and A. Muñoz Sudupe, Phys. Lett. B **441**, 330 (1998), cond-mat/9805022.

[25] H.G. Ballesteros, L.A. Fernández, V. Martín-Mayor, A. Muñoz Sudupe, G. Parisi and J.J. Ruiz-Lorenzo, J. Phys. A **32**, 1 (1999), cond-mat/9805125.

[26] M.M. Tsypin and H.W.J. Blöte, Probability distribution of the order parameter for the 3D Ising model universality class: A high precision Monte Carlo study. Preprint, cond-mat/9909343.

[27] S.Y. Zinn, S.-N. Lai and M.E. Fisher, Phys. Rev. E **54**, 1176 (1996).

[28] A. Pelissetto and E. Vicari, Nucl. Phys. B **519**, 626 (1998), cond-mat/9711078.

[29] A. Pelissetto and E. Vicari, Nucl. Phys. B **522**, 605 (1998), cond-mat/9801098.

[30] A.I. Sokolov and E.V. Orlov, Phys. Rev. B **58**, 2395 (1998), cond-mat/9804008.

[31] J.–K. Kim, The critical renormalized coupling constants in the symmetric phase of the Ising models. Preprint, cond-mat/9905138.

[32] S. Caracciolo, R.G. Edwards, A. Pelissetto and A.D. Sokal, Phys. Rev. Lett. **75**, 1891 (1995), hep-lat/9411009.

[33] S. Caracciolo, R.G. Edwards, T. Mendes, A. Pelissetto and A.D. Sokal, Nucl. Phys. B (Proc. Suppl.) **47**, 763 (1996), hep-lat/9509033.

[34] G. Mana, A. Pelissetto and A.D. Sokal, Phys. Rev. D **55**, 3674 (1997), hep-lat/9610021.

[35] J. Balog and M. Niedermaier, Nucl. Phys. B **500**, 421 (1997), hep-th/9612039.

[36] J. Balog, M. Niedermaier, F. Niedermayer, A. Patrascioiu, E. Seiler and P. Weisz, Comparison of the $O(3)$ bootstrap σ-model with the lattice regularization at low energies. Preprint, hep-lat/9903036.

[37] M. Caselle, R. Tateo and S. Vinti, Universal amplitudes in the 2D four state Potts model. Preprint, cond-mat/9902146. Nucl. Phys. B, in press.

[38] G. Delfino, G.T. Barkema and J. Cardy, Susceptibility amplitude ratios in the two-dimensional Potts model and percolation. Preprint, cond-mat/9908453.

[39] C.M. Naón, J. Phys. A **22**, 2877 (1989)

[40] A.J. Liu and M.E. Fisher, Physica A **156**, 35 (1989).

[41] J.-K. Kim and A. Patrascioiu, Phys. Rev. D **47**, 2588 (1993).

[42] C. Gutsfeld, J. Küster and G. Münster, Nucl. Phys. B **479**, 654 (1996), cond-mat/9606091.

[43] S.-Y. Zinn and M.E. Fisher, Physica A **226**, 168 (1996).

[44] R. Guida and J. Zinn-Justin, Nucl. Phys. B **489**, 626 (1997), hep-th/9610223.

[45] M. Caselle and M. Hasenbusch, J. Phys. A **30**, 4963 (1997), hep-lat/9701007.

[46] A. Pelissetto and E. Vicari, Low-temperature effective potential of the Ising model. Preprint, cond-mat/9805317.

[47] M. Weigel and W. Janke, Phys. Rev. Lett. **82**, 2318 (1999), cond-mat/9809253.

[48] P. Butera and M. Comi, Phys. Rev. B **58**, 11552 (1998), hep-lat/9805025.

[49] A.I. Sokolov, E.V. Orlov, V.A. Ul'kov and S.S. Kashtanov, Phys. Rev. E **60**, 1344 (1999), hep-th/9810082.

[50] A.C. Petkou and N.D. Vlachos, Phys. Lett. B **446**, 306 (1999), hep-th/9803146.

[51] E. Luitjen, K. Binder and H.W.J. Blöte, Eur. Phys. J. B **9**, 289 (1999), cond-mat/9901042.

[52] T.T. Wu, B.M. McCoy, C.A. Tracy and E. Barouch, Phys. Rev. B **13**, 316 (1976).

[53] P. Di Francesco, H. Saleur and J.-B. Zuber, Nucl. Phys. B **290** [FS20] (1987) 527.

[54] P. Di Francesco, H. Saleur and J.-B. Zuber, Europhys. Lett. **5** (1988) 95.

[55] J.L. Cardy, Phys. Rev. Lett. **60**, 2709 (1988).

[56] J.L. Cardy, J. Phys. A **21**, L797 (1988).

[57] J.L. Cardy and H. Saleur, J. Phys. A **22**, L601 (1989).

[58] S. Caracciolo, A. Pelissetto and A.D. Sokal, J. Phys. A **23**, L969 (1990).

[59] J.L. Cardy and G. Mussardo, Nucl. Phys. B **410**, 451 (1993), hep-th/9306028.

[60] J.L. Cardy and A.J. Guttmann, J. Phys. A **26**, 2485 (1993), cond-mat/9303035.

[61] A.V. Smilga, Phys. Rev. D **55**, R443 (1997).

[62] G. Delfino, Phys. Lett. B **419**, 291 (1998), hep-th/9710019.

[63] G. Delfino and J.L. Cardy, Nucl. Phys. B **519**, 551 (1998), hep-th/9712111.

[64] K. Binder, Z. Phys. B **43**, 119 (1981).

[65] C.M. Newman, Z. Wahr. verw. Geb. **33**, 75 (1975).

[66] J. Bricmont, J. Stat. Phys. **17**, 289 (1977).

[67] C.M. Newman, Commun. Math. Phys. **41**, 1 (1975).

[68] S.B. Shlosman, Commun. Math. Phys. **102**, 679 (1986).

[69] M. Lüscher, P. Weisz and U. Wolff, Nucl. Phys. B **359**, 221 (1991).

[70] J.-K. Kim, Phys. Rev. Lett. **70**, 1735 (1993).

[71] S. Caracciolo, R.G. Edwards, S.J. Ferreira, A. Pelissetto and A.D. Sokal, Phys. Rev. Lett. **74**, 2969 (1995), hep-lat/9409004.

[72] S. Caracciolo, A. Pelissetto and A.D. Sokal, in preparation.

[73] V. Privman and M.E. Fisher, Phys. Rev. B **30**, 322 (1984).

[74] J.L. Cardy, J. Phys. A **17**, L385 (1984).

[75] J. Salas and A.D. Sokal, J. Stat. Phys. **87**, 1 (1997), hep-lat/9605018.

[76] J. Salas and A.D. Sokal, J. Stat. Phys. **85**, 297 (1996), hep-lat/9511022.

[77] J. Salas and A.D. Sokal, J. Stat. Phys. **88**, 567 (1997), hep-lat/9607030.

[78] J. Salas and A.D. Sokal, J. Stat. Phys. **92**, 729 (1998), cond-mat/9801079.

[79] S.J. Ferreira and A.D. Sokal, J. Stat. Phys. **96**, 461 (1999), cond-mat/9811345.

[80] J.–K. Kim, private communication.

[81] G. Kamieniarz and H.W.J. Blöte, J. Phys. A **26**, 201 (1993).

[82] G.A. Baker Jr. and N. Kawashima, J. Phys. A **29**, 7183 (1996).

[83] G.A. Baker Jr., J. Stat. Phys. **77**, 955 (1994).

[84] P. Butera and N. Comi, Phys. Rev. B **54**, 15828 (1996), hep-lat/9710092.

[85] J.C. LeGuillou and J. Zinn-Justin, Phys. Rev. B **21**, 3976 (1980).

[86] C.M. Bender and S. Boettcher, Phys. Rev. D **48**, 4919 (1993), hep-th/9311060.

[87] C.M. Bender and S. Boettcher, Phys. Rev. D **51**, 1875 (1995), hep-th/9405043.

[88] R.H. Swendsen and J.-S. Wang, Phys. Rev. Lett. **58**, 86 (1987).

[89] R.G. Edwards and A.D. Sokal, Phys. Rev. D **38**, 2009 (1988).

[90] A.D. Sokal, in *Functional Integration: Basics and Applications* (1996 Cargèse summer school), ed. C. DeWitt-Morette, P. Cartier and A. Folacci (Plenum, New York, 1997).

[91] P.W. Kasteleyn and C.M. Fortuin, J. Phys. Soc. Japan **26** (Suppl.), 11 (1969).

[92] C.M. Fortuin and P.W. Kasteleyn, Physica **57**, 536 (1972).

[93] C.M. Fortuin, Physica **58**, 393 (1972); **59**, 545 (1972).

[94] N. Madras and A.D. Sokal, J. Stat. Phys. **50**, 109 (1988).

[95] X.–J. Li and A.D. Sokal, Phys. Rev. Lett. **63**, 827 (1989).

[96] H.G. Ballesteros, L.A. Fernández, V. Martín-Mayor, A. Muñoz Sudupe, G. Parisi and J.J. Ruiz-Lorenzo, J. Phys. A **30**, 8379 (1998), cond-mat/9707179; and private communication.

[97] U. Wolff, Phys. Rev. Lett. **62**, 3834 (1989).

[98] V. Privman in *Finite Size Scaling and Numerical Simulation of Statistical Systems*, edited by V. Privman (World Scientific, Singapore, 1990).

[99] H. Guo and D. Jasnow, Phys. Rev. B **35**, 1846 (1987); **39**, 753 (E) (1989).

[100] A. Aharony and M.E. Fisher, Phys. Rev. B **27**, 4394 (1983).

[101] S. Gartenhaus and W.S. McCullough, Phys. Rev. B **38**, 11688 (1988).

[102] B. Nickel, J. Phys. A: Math. Gen. **32**, 3889 (1999).

[103] B. Nickel, Addendum to "On the singularity structure of the 2-d Ising model susceptibility". University of Guelph preprint, June 1999.

[104] A. Pelissetto, private communication (May 1999).

[105] F.J. Wegner, Phys. Rev. B **5**, 4529 (1972).

[106] F.J. Wegner, in *Phase Transitions and Critical Phenomena*, vol. 6, edited by C. Domb and M.S. Green (Academic Press, London, 1976).

[107] J. Salas and A.D. Sokal, in preparation.

[108] C.M. Newman, private communication (1999).

[109] C.M. Newman, Commun. Math. Phys. **74**, 119 (1980).

[110] C.M. Newman, Commun. Math. Phys. **91**, 75 (1983).

[111] M. den Nijs, M.P. Nightingale and M. Schick, Phys. Rev. **B26**, 2490 (1982).

[112] J.K. Burton Jr. and C.L. Henley, J. Phys. **A30**, 8385 (1997), cond-mat/9708171.

[113] S. Caracciolo, A. Pelissetto, J. Salas and A.D. Sokal, work in progress.

[114] C. Itzykson and J.-M. Drouffe, *Statistical Field Theory* (Cambridge University Press, Cambridge, 1989), Vol. 2.

[115] I.S. Gradshteyn and I.M. Ryzhik, *Table of Integrals, Series and Products* (Academic Press, New York, 1965).

L	MCS	χ	F	ξ
4	2.10	12.1825 ± 0.0065	0.40470 ± 0.00080	3.8146 ± 0.0051
6	2.70	24.9443 ± 0.0130	0.77280 ± 0.00130	5.5927 ± 0.0063
8	2.70	41.4214 ± 0.0228	1.25230 ± 0.00210	7.3998 ± 0.0084
12	3.25	84.3329 ± 0.0454	2.53300 ± 0.00380	10.9783 ± 0.0114
16	3.25	139.5946 ± 0.0786	4.18240 ± 0.00630	14.5832 ± 0.0154
24	4.00	284.0239 ± 0.1525	8.49420 ± 0.01180	21.8170 ± 0.0212
32	4.00	469.7765 ± 0.2612	14.08820 ± 0.01970	29.0118 ± 0.0288
48	5.00	955.5980 ± 0.4966	28.66410 ± 0.03650	43.4737 ± 0.0395
64	5.00	1580.9962 ± 0.8442	47.39310 ± 0.06100	57.9660 ± 0.0535
96	6.40	3214.3979 ± 1.5807	96.39390 ± 0.11180	86.9125 ± 0.0728
128	6.40	5322.9013 ± 2.6899	159.27970 ± 0.18690	116.0034 ± 0.0990
192	7.10	10817.0940 ± 5.3669	324.09120 ± 0.36560	173.8830 ± 0.1434
256	7.10	17898.9900 ± 9.0732	536.06730 ± 0.61150	231.8851 ± 0.1940
512	8.10	60184.2200 ± 29.9896	1804.17680 ± 1.96390	463.5381 ± 0.3745

Table 1: Values of the principal static observables for the 2D Ising model at criticality. For each lattice size L we show the number of measurements (= Swendsen-Wang iterations after the discard interval) in units of 10^6 (MCS), the susceptibility χ, the Fourier-transformed correlation function $F = \widetilde{G}(2\pi/L, 0)$, and the second-moment correlation length ξ.

L	V_4	V_6	V_8	V_{10}	V_{12}
4	1.14827 ± 0.00041	1.38285 ± 0.00108	1.7100 ± 0.0021	2.1505 ± 0.0037	2.7358 ± 0.0061
6	1.15753 ± 0.00038	1.41690 ± 0.00102	1.7941 ± 0.0021	2.3258 ± 0.0037	3.0687 ± 0.0064
8	1.16042 ± 0.00039	1.42853 ± 0.00106	1.8247 ± 0.0022	2.3930 ± 0.0040	3.2026 ± 0.0069
12	1.16460 ± 0.00037	1.44302 ± 0.00103	1.8600 ± 0.0021	2.4675 ± 0.0039	3.3481 ± 0.0069
16	1.16586 ± 0.00038	1.44774 ± 0.00106	1.8721 ± 0.0022	2.4942 ± 0.0041	3.4020 ± 0.0073
24	1.16672 ± 0.00036	1.45126 ± 0.00100	1.8815 ± 0.0021	2.5151 ± 0.0039	3.4447 ± 0.0069
32	1.16756 ± 0.00037	1.45400 ± 0.00103	1.8880 ± 0.0022	2.5288 ± 0.0040	3.4717 ± 0.0072
48	1.16769 ± 0.00034	1.45475 ± 0.00094	1.8903 ± 0.0020	2.5342 ± 0.0037	3.4830 ± 0.0066
64	1.16777 ± 0.00034	1.45494 ± 0.00097	1.8907 ± 0.0020	2.5353 ± 0.0038	3.4854 ± 0.0068
96	1.16769 ± 0.00031	1.45493 ± 0.00088	1.8910 ± 0.0019	2.5363 ± 0.0035	3.4880 ± 0.0062
128	1.16763 ± 0.00032	1.45469 ± 0.00090	1.8904 ± 0.0019	2.5351 ± 0.0036	3.4857 ± 0.0063
192	1.16764 ± 0.00031	1.45474 ± 0.00087	1.8906 ± 0.0018	2.5356 ± 0.0035	3.4871 ± 0.0062
256	1.16777 ± 0.00031	1.45514 ± 0.00089	1.8914 ± 0.0019	2.5371 ± 0.0035	3.4895 ± 0.0063
512	1.16782 ± 0.00030	1.45526 ± 0.00086	1.8917 ± 0.0018	2.5376 ± 0.0034	3.4906 ± 0.0061
∞	1.1679229(47)	1.4556491(72)	1.89252(18)	2.53956(34)	

L	V_{14}	V_{16}	V_{18}	V_{20}
4	3.509 ± 0.010	4.527 ± 0.015	5.866 ± 0.022	7.626 ± 0.033
6	4.105 ± 0.010	5.551 ± 0.017	7.575 ± 0.027	10.414 ± 0.042
8	4.356 ± 0.012	6.006 ± 0.019	8.374 ± 0.031	11.791 ± 0.049
12	4.628 ± 0.012	6.496 ± 0.020	9.241 ± 0.033	13.300 ± 0.054
16	4.731 ± 0.012	6.688 ± 0.021	9.589 ± 0.035	13.921 ± 0.058
24	4.814 ± 0.012	6.843 ± 0.020	9.874 ± 0.034	14.436 ± 0.057
32	4.864 ± 0.012	6.936 ± 0.021	10.040 ± 0.036	14.732 ± 0.060
48	4.887 ± 0.012	6.979 ± 0.020	10.123 ± 0.033	14.883 ± 0.056
64	4.892 ± 0.012	6.990 ± 0.020	10.143 ± 0.034	14.922 ± 0.058
96	4.898 ± 0.011	7.001 ± 0.019	10.165 ± 0.031	14.965 ± 0.053
128	4.894 ± 0.011	6.995 ± 0.019	10.154 ± 0.032	14.947 ± 0.054
192	4.897 ± 0.011	7.001 ± 0.018	10.166 ± 0.031	14.970 ± 0.053
256	4.901 ± 0.011	7.006 ± 0.019	10.175 ± 0.032	14.982 ± 0.054
512	4.903 ± 0.011	7.011 ± 0.018	10.183 ± 0.031	14.997 ± 0.052

Table 2: Values of the ratios $V_{2n} = \langle \mathcal{M}^{2n} \rangle / \langle \mathcal{M}^2 \rangle^n$ for the 2D Ising model at criticality, as a function of the lattice size L. The row $L = \infty$ shows the theoretical predictions (2.17)/(2.20)/(2.21)/(2.22) for V_4, V_6, V_8 and V_{10}, respectively; they are exact except for a numerical integration, the error bars of which are given in parentheses.

L	EIM	ξ
12	0.4	10.976 ± 0.015
16	0.4	14.575 ± 0.019
24	0.6	21.791 ± 0.026
32	0.4	29.089 ± 0.038
48	0.6	43.448 ± 0.043
64	0.6	57.877 ± 0.056
96	0.6	86.87 ± 0.11
128	0.6	115.87 ± 0.12
192	0.5	174.06 ± 0.21
256	0.6	231.84 ± 0.31
512	0.7	464.8 ± 0.5

Table 3: Values of the correlation length ξ for the 2D Ising model at $\beta = \beta_c$ obtained by Ballesteros *et al.* [96]. For each lattice size L we also show the number of "effectively independent measurements" in units of 10^6 (EIM).

L	ξ	ξ/L	ξ'/L
4	3.8146 ± 0.0051	0.95365 ± 0.00128	0.85859 ± 0.00115
6	5.5927 ± 0.0063	0.93212 ± 0.00105	0.89011 ± 0.00100
8	7.3998 ± 0.0084	0.92497 ± 0.00105	0.90138 ± 0.00102
12	10.9775 ± 0.0091	0.91479 ± 0.00076	0.90437 ± 0.00075
16	14.5799 ± 0.0120	0.91125 ± 0.00075	0.90540 ± 0.00074
24	21.8066 ± 0.0164	0.90861 ± 0.00068	0.90602 ± 0.00068
32	29.0400 ± 0.0230	0.90750 ± 0.00072	0.90604 ± 0.00072
48	43.4619 ± 0.0291	0.90546 ± 0.00061	0.90481 ± 0.00061
64	57.9235 ± 0.0387	0.90506 ± 0.00060	0.90469 ± 0.00060
96	86.8996 ± 0.0607	0.90520 ± 0.00063	0.90504 ± 0.00063
128	115.9494 ± 0.0764	0.90585 ± 0.00060	0.90576 ± 0.00060
192	173.9393 ± 0.1184	0.90593 ± 0.00062	0.90589 ± 0.00062
256	231.8724 ± 0.1645	0.90575 ± 0.00064	0.90573 ± 0.00064
512	463.9916 ± 0.2997	0.90623 ± 0.00059	0.90623 ± 0.00059
∞		0.9050488	0.9050488

Table 4: Values of the correlation length ξ for the 2D Ising model at $\beta = \beta_c$ coming from merging our data (see Table 1) with that of Ballesteros *et al.* [96] (see Table 3). The second column shows the ratio ξ/L, and the last column shows the ratio ξ'/L. The last row ($L = \infty$) shows the theoretical prediction (2.14) for the infinite-volume limit of the ratios ξ/L and ξ'/L.

$2n$	Type	V_{2n}^{∞}	B	Δ	L_{min}	χ^2	DF	level
4	C	1.16770 ± 0.00011			32	0.48	7	100%
	P	1.16777 ± 0.00013	-0.477 ± 0.228	2.007 ± 0.223	8	1.53	9	100%
	T	1.1679229 ± 0.0000047						
6	C	1.45484 ± 0.00032			32	1.09	7	99%
	P	1.45517 ± 0.00037	-1.387 ± 0.476	1.901 ± 0.160	8	1.66	9	100%
	T	1.4556491 ± 0.0000072						
8	C	1.89090 ± 0.00071			48	0.48	6	100%
	P	1.89163 ± 0.00079	-3.037 ± 0.827	1.834 ± 0.127	8	1.86	9	99%
	T	1.89252 ± 0.00018						
10	C	2.53593 ± 0.00135			48	0.69	6	99%
	P	2.53769 ± 0.00151	-5.915 ± 1.341	1.784 ± 0.106	8	2.06	9	99%
	T	2.53956 ± 0.00034						
12	C	3.48720 ± 0.00241			48	0.99	6	99%
	P	3.49106 ± 0.00273	-10.819 ± 2.112	1.742 ± 0.091	8	2.29	9	99%
14	C	4.89621 ± 0.00418			48	1.37	6	97%
	P	4.90419 ± 0.00479	-19.019 ± 3.264	1.705 ± 0.080	8	2.56	9	98%
16	C	6.99812 ± 0.00716			48	1.83	6	93%
	P	7.01407 ± 0.00827	-32.544 ± 4.984	1.670 ± 0.072	8	2.86	9	97%
18	C	10.16503 ± 0.01303			64	0.97	5	97%
	P	10.19047 ± 0.01416	-54.624 ± 7.553	1.635 ± 0.065	8	3.23	9	95%
20	C	14.96506 ± 0.02199			64	1.16	5	95%
	P	15.01380 ± 0.02411	-90.377 ± 11.374	1.601 ± 0.059	8	3.69	9	93%

Table 5: Values of the infinite-volume-limit ratios $V_{2n} = \langle \mathcal{M}^{2n} \rangle / \langle \mathcal{M}^2 \rangle^n$ for the 2D Ising model at criticality. For each n we show the results of two different types of fits: to a constant $V_{2n} = V_{2n}^{\infty}$ (C), and to a constant plus a power-law correction-to-scaling term $V_{2n} = V_{2n}^{\infty} + B_{2n} L^{-\Delta}$ (P). We also show, for comparison, the theoretical prediction itself (T) for $2n = 4, 6, 8, 10$. The values of L_{min}, χ^2, the number of degrees of freedom (DF) and the confidence level are also shown.

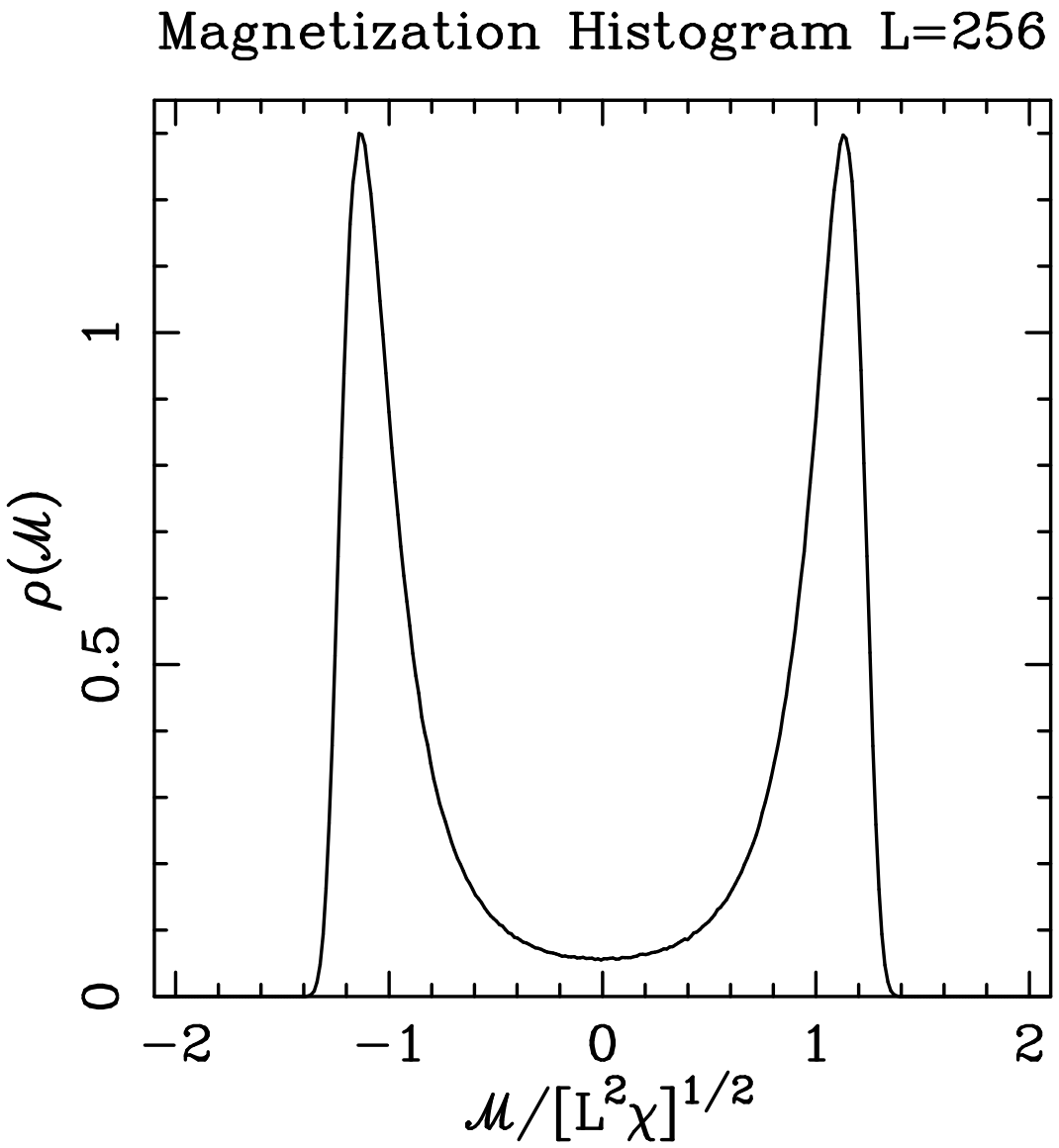

Figure 1: Magnetization histogram of the 2D Ising model at $\beta = \beta_c$ for $L = 256$. The histogram is normalized such that the area enclosed is equal to unity.